



**Some parts of this thesis may have been removed for copyright restrictions.**

If you have discovered material in AURA which is unlawful e.g. breaches copyright, (either yours or that of a third party) or any other law, including but not limited to those relating to patent, trademark, confidentiality, data protection, obscenity, defamation, libel, then please read our [Takedown Policy](#) and [contact the service](#) immediately

THE DIAGENESIS AND PALAEOMAGNETISM OF PERMIAN AND TRIASSIC  
SEDIMENTS FROM CENTRAL SPAIN.

VOL II

AMANDA ROSE TURNER

Doctor of Philosophy

THE UNIVERSITY OF ASTON IN BIRMINGHAM

October 1988

This copy of the thesis has been supplied on condition that anyone who consults it is understood to recognise that its copyright rests with its author and that no quotation from the thesis and no information derived from it may be published without the author's prior, written consent.

LIST OF CONTENTS

VOLUME II

		<u>PAGE</u>
Title Page.....		1
List of Contents.....		2
List of Tables.....		3
List of Figures.....		4
List of Plates.....		5
Photographic Plates.....		7
APPENDICES.....		55
APPENDIX I	Techniques Used on Samples.....	55
APPENDIX II	Sample Preparation for Palaeomagnetic Analysis..	60
APPENDIX III	Staining a Thin Section.....	61
APPENDIX IV	Classification of Terrigenous Sandstones.....	62
APPENDIX V	(a) The Preparation of Orientated Clay Mineral Specimens for X-Ray Diffraction Analysis by a Suction-Onto-Ceramic Tile Method.....	63
	(b) Identification of X-ray Diffraction Peaks..	64
APPENDIX VI	Types of Magnetization.....	65
APPENDIX VII	Point Count Analysis.....	66
APPENDIX VIII	Stability Index.....	73

LIST OF TABLES

		<u>PAGE</u>
Table 9.1	Listing of techniques used on each sample.	55
Table 9.2	Etching of staining characteristics of Carbonate Minerals.	61
Table 9.3	Key to identification of X-ray diffractogram plate.	64
Table 9.4	Types of Magnetization.	65
Table 9.5	Point Count Analysis for the Autunian of Palmaces.	66
Table 9.6	Point Count Analysis for the Saxonian.	67
Table 9.7	Point Count Analysis for the Lower Buntsandstein.	68
Table 9.8	Point Count Analysis for the Upper Buntsandstein.	70
Table 9.9	Point Count Analysis for the Muschelkalk of Riba de Santuiste.	72
Table 9.10	Stability Index (S.I.).	73

LIST OF FIGURES

	<u>PAGE</u>
Fig. 9.1 Shows how sample is orientated in the field and how it is prepared for palaeomagnetic measurement.	60
Fig. 9.2 Classification of terrigenous sandstones (after Dott, 1964).	62
Fig. 9.3 Suction-out-ceramic disc method of sample preparation.	63

LIST OF PLATES

VOL II

PAGE

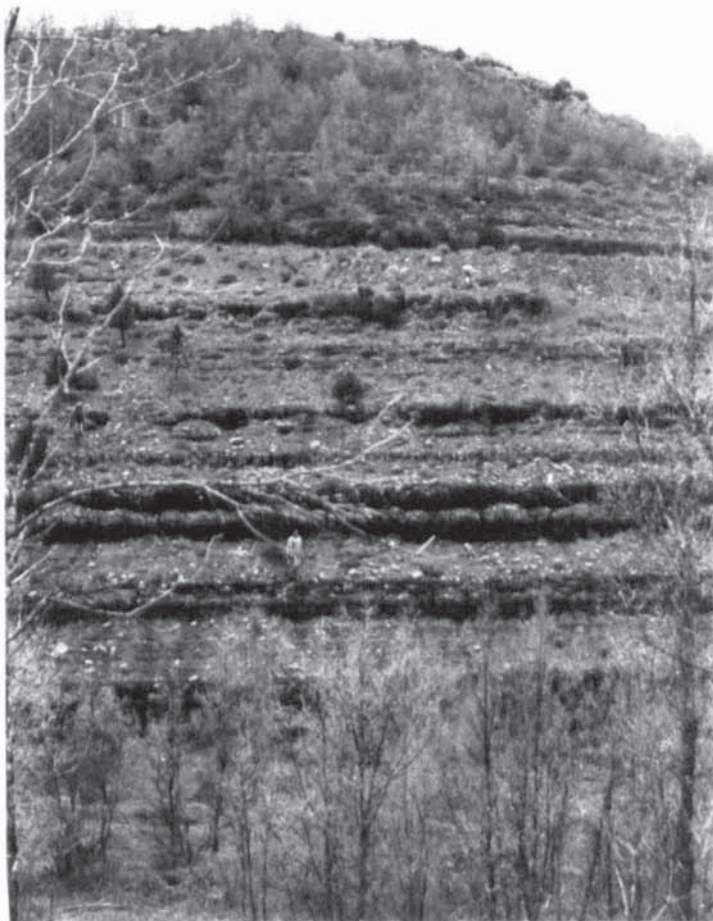
Plate 2.1	Field photographs of the Autunian from the Rillo de Gallo section.	8
Plate 2.2	Photomicrographs showing diagenetic features in the Autunian of Rillo de Gallo.	10
Plate 2.3	Photomicrographs showing diagenetic features in the Autunian of Rillo de Gallo.	12
Plate 3.1	Field photographs of the Autunian from the Palmaces section.	14
Plate 3.2	Photomicrographs showing diagenetic features in the Autunian of Palmaces.	16
Plate 3.3	Photomicrographs showing diagenetic features in the Autunian of Palmaces.	18
Plate 4.1	Field photograph of the Saxonian from the Torres de Albarracin section.	20
Plate 4.2	Photomicrographs showing diagenetic features in the Saxonian of Pozo Nuncio and Torres de Albarracin.	22
Plate 4.3	Photomicrographs showing diagenetic features in the Saxonian of Pozo Nuncio and Torres de Albarracin.	24
Plate 4.4	Photomicrographs showing diagenetic features in the Saxonian of Torres de Albarracin and Barranco de la Hoz.	26
Plate 4.5	Photomicrographs showing diagenetic features in the Saxonian of Barranco de la Hoz and Pozo Nuncio.	28
Plate 5.1	Field photographs of the Lower Buntsandstein from the Hoz del Gallo and Rillo de Gallo section.	30
Plate 5.2	Photomicrographs showing diagenetic features in the Lower Buntsandstein of Hoz del Gallo.	32

	<u>PAGE</u>
Plate 5.3 Photomicrographs showing diagenetic features of the Lower Buntsandstein from the Hoz del Gallo and Rillo de Gallo.	34
Plate 5.4 Photomicrographs showing diagenetic features of the Lower Buntsandstein from Hoz del Gallo.	36
Plate 6.1 Field photographs from the Upper Buntsandstein of the Rillo de Gallo and Rio Arandilla sections.	38
Plate 6.2 Photomicrographs showing diagenetic features of the Upper Buntsandstein from Rillo de Gallo and Rio Arandilla.	40
Plate 6.3 Photomicrographs showing diagenetic features of the Upper Buntsandstein from Rillo de Gallo.	42
Plate 6.4 Photomicrographs showing diagenetic features of the Upper Buntsandstein from Rillo de Gallo and Rio Arandilla.	44
Plate 7.1 Field photographs of the Muschelkalk and Keuper sections of Castellar de la Muella, Rillo de Gallo and Teroleja.	46
Plate 7.2 Photomicrographs showing diagenetic features in the Muschelkalk.	48
Plate 7.3 Photomicrographs showing diagenetic features in the Muschelkalk.	50
Plate 7.4 Photomicrographs showing diagenetic features in the Muschelkalk and Keuper.	52
Plate 7.5 Photomicrographs showing diagenetic features in the Muschelkalk and Keuper.	54

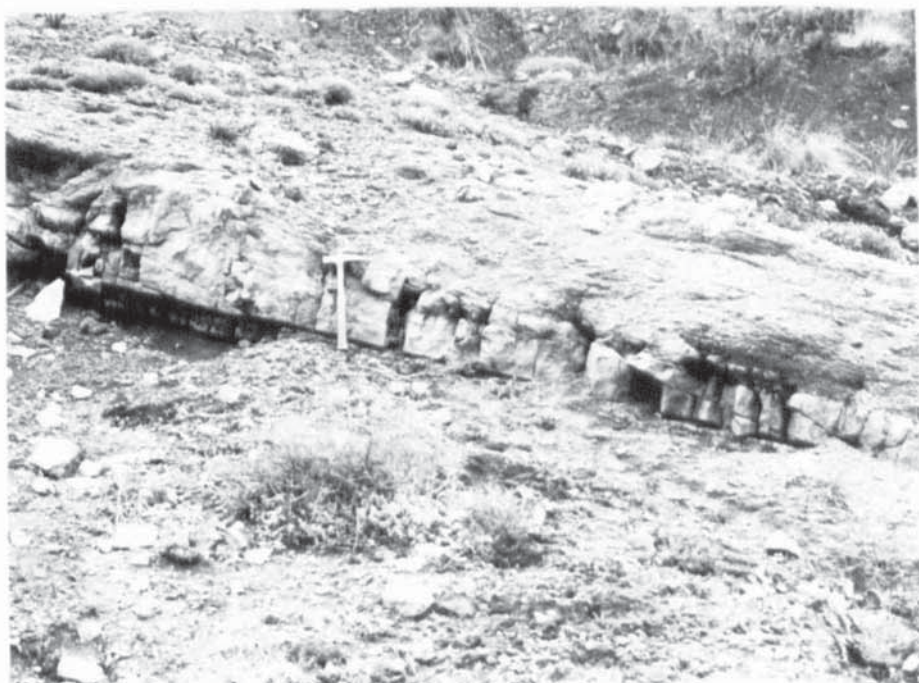
PLATE 2.1

- a) Cliff section at Rillo de Gallo looking SW  
Gently dipping beds of upper part of subunit  
E2 of the Capas de la Ermita, Autunian  
facies.
  
- b) Resistant, volcaniclastic bed in subunit E2  
of Capas de la Ermita, Autunian facies.  
Rillo de Gallo section (site of sample RG11).

**Plate 2.1**



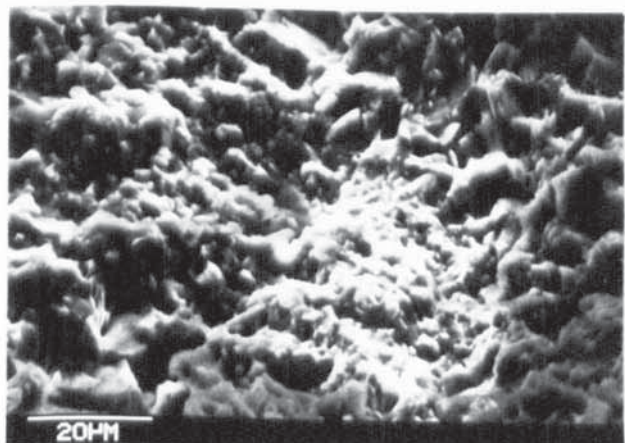
**a**



**b**

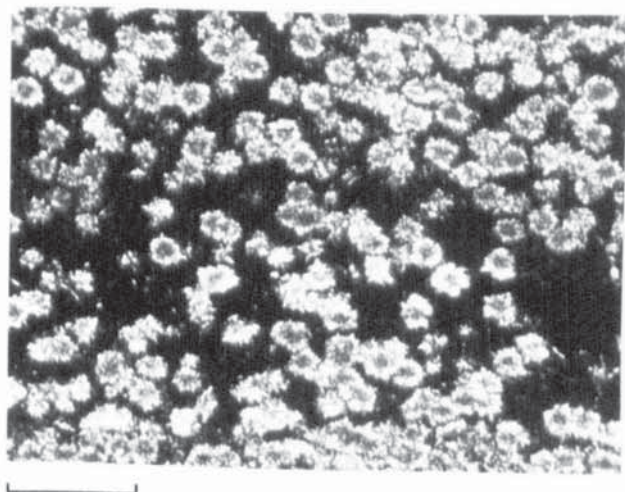
PLATE 2.2

- a) RG2: Cryptocrystalline silica matrix of devitrified tuff coated, in places, by authigenic clays.  
Viewed under SEM. Scale bar = 20  $\mu\text{m}$
- b) RG4: Severely corroded quartz grain in siliceous and clay rich matrix.  
Scale bar = 0.1mm
- c) RG13: Abundant spherulites indicate devitrification of a silica rich tuff.  
Scale bar = 0.5mm
- d) RG2: Potassium feldspar replaced by kaolinite in the grain core.  
Scale bar = 0.1mm
- e) RG2: Muscovite mica showing replacement by kaolinite at grain margins.  
Scale bar = 0.2mm
- f) RG6: Non-ferroan calcite patch containing haematite (evidence of dedolomitization?) in siliceous matrix.  
Scale bar = 0.2mm

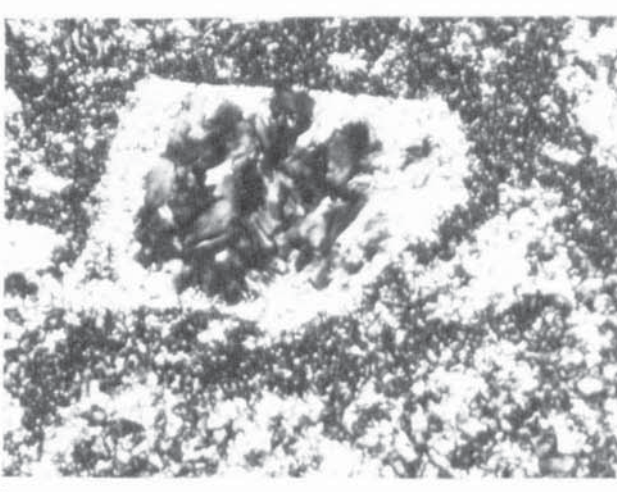


a

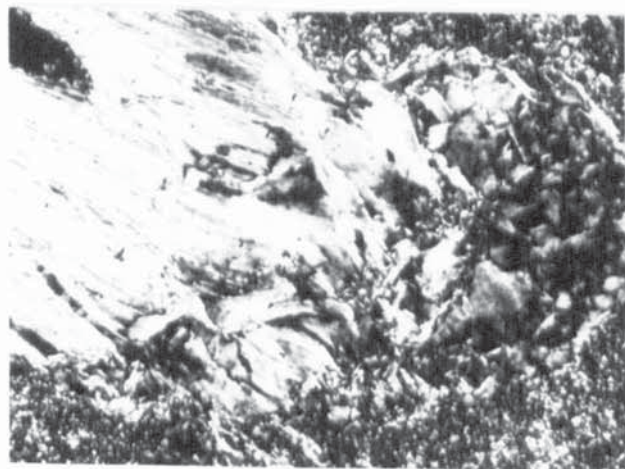
b



c



d



e

f

PLATE 2.3

- a) RG6: Strong evidence for dedolomitization is shown by the rhombic outlines of calcite and thick haematite linings. Reflect ferroan dolomite is sometimes associated with this haematite.  
Scale bar = 0.2mm
- b) RG14: Secondary porosity in the form of subhedral vugs lined by fine grained haematite.  
Scale bar = 0.2mm
- c) RG6: Coarse rounded (detrital haematite in fine grained siliceous matrix.  
Scale bar = 0.1mm
- d) RG5: authigenic, lath like, crystal of ilmenite within mica parallel with mica cleavage.  
Viewed under reflected light.  
Scale bar = 70 $\mu$ m
- e) RG10: Framboidal aggregates of haematite.  
Pseudomorphs after pyrite?  
Scale bar = 0.7mm
- f) RG4: Fine grained haematite infills secondary pores. Note rhombic outline of many of the pores.  
Scale bar = 0.2mm

Plate 2.3

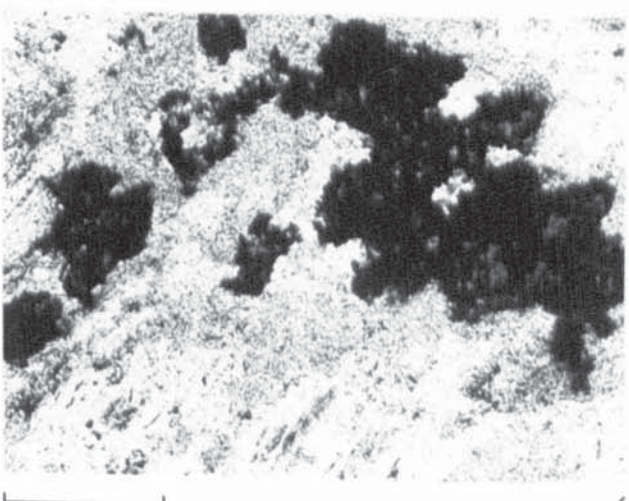
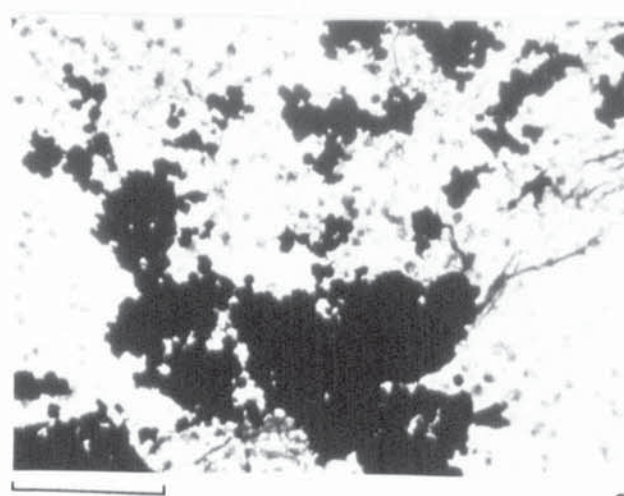
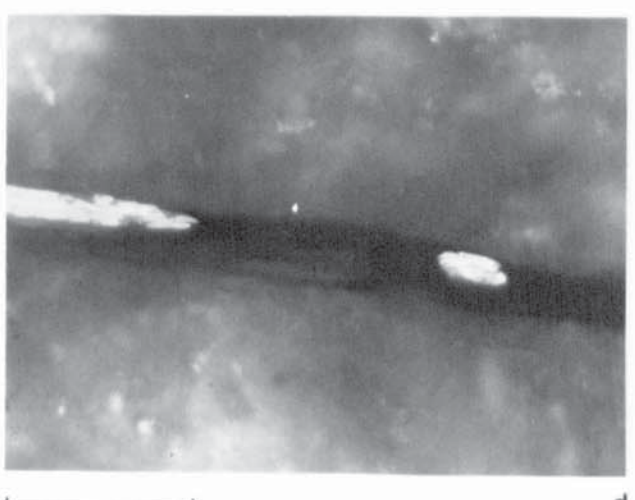
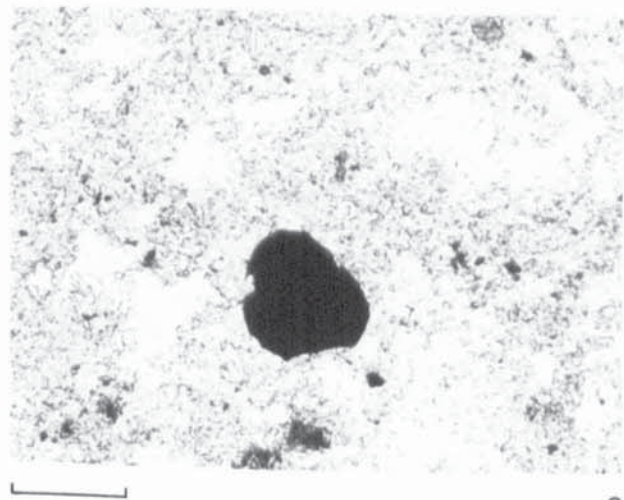
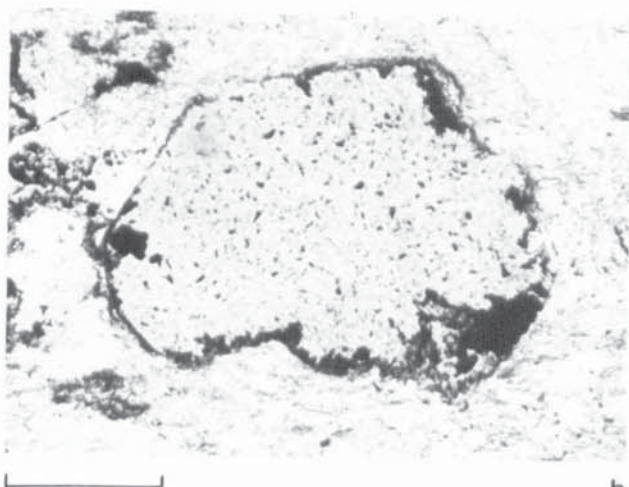
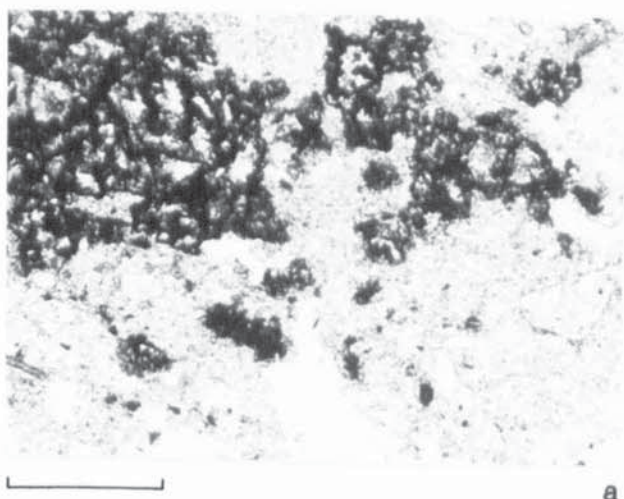


PLATE 3.1

- a) View northeast across part of the Palmaces Reservoir showing gently dipping Permian and Triassic sediments. Samples P1 and P10 were taken from the deposits in the centre/left of this photograph (see Fig. 3.1).
- b) View southwest demonstrating the unconformable contact between the Permian and overlying Triassic, Buntsandstein facies in the Palmaces section.

**Plate 3.1**

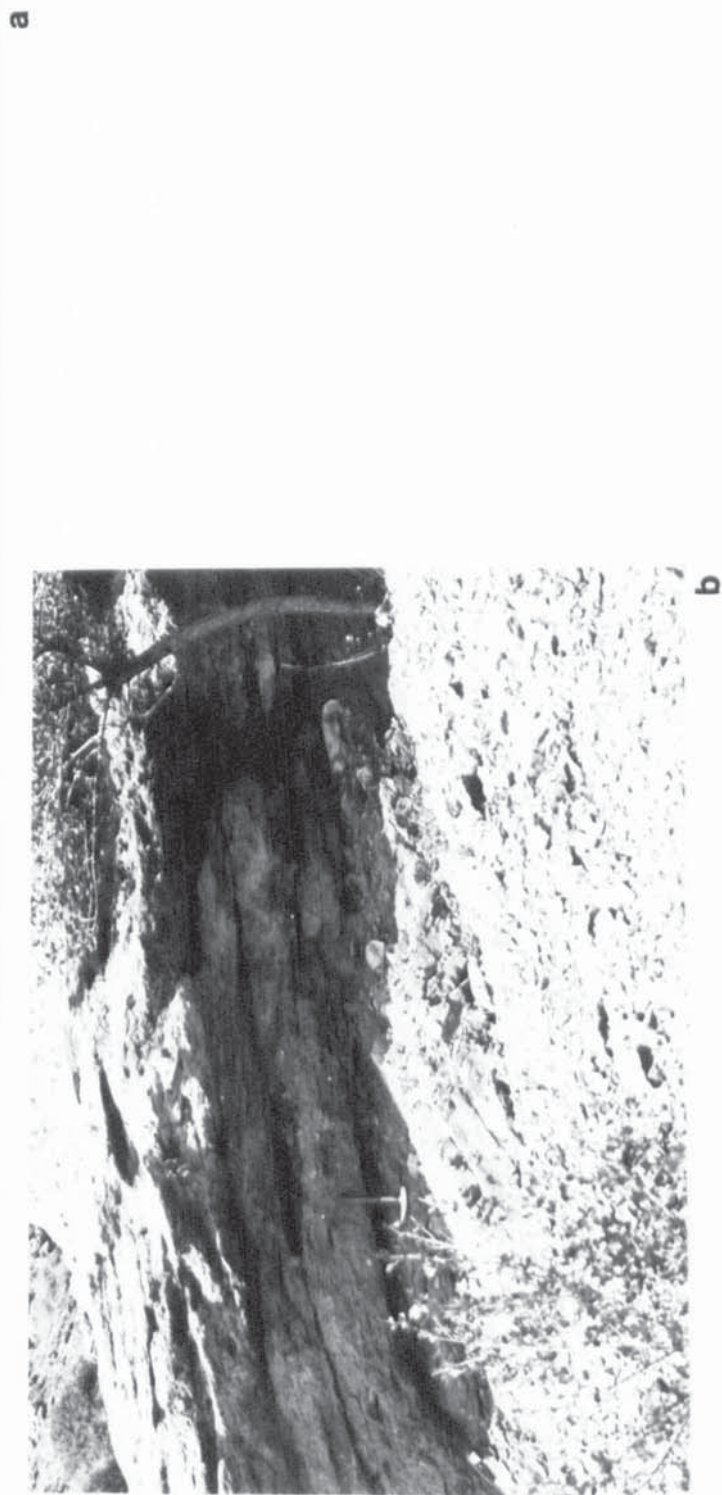


PLATE 3.2

- a) P5: Partial replacement of quartz grains by aggressive carbonate cement.  
Scale bar = 0.15mm
- b) P5: Replacement of feldspar core by authigenic kaolinite.  
Scale bar = 0.1mm
- c) P5: Replacement of rock fragment? by iron oxide and clays.  
Scale bar = 0.15mm
- d) P3: Tangentially orientated platelets of allogenic clay.  
Viewed under S.E.M.  
Scale bar = 10 $\mu$ m
- e) P7: Replacement of rock fragment? by authigenic clay.  
Scale bar = 0.1mm
- f) P7: Syntaxial overgrowth of authigenic quartz. This clearly pre-dates the carbonate cement seen just above.  
Scale bar = 0.15mm

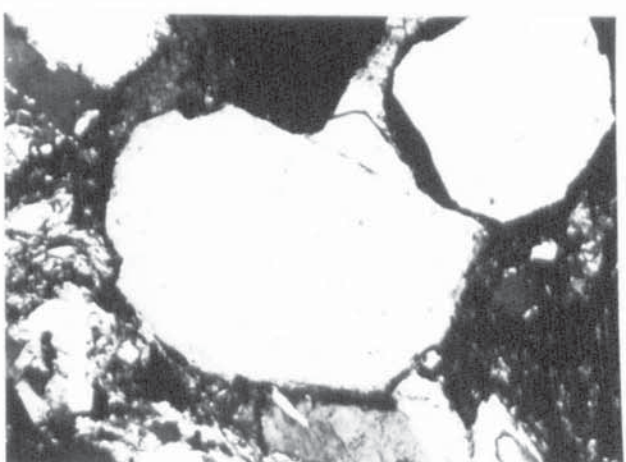
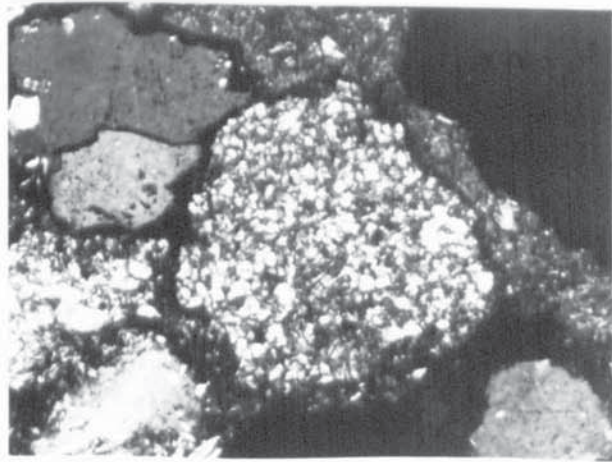
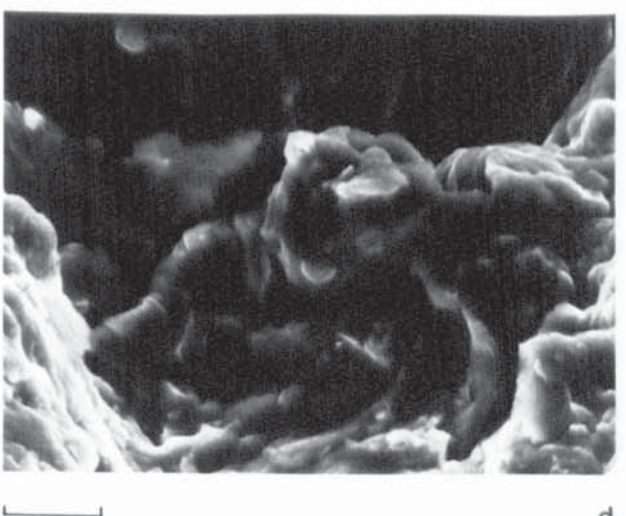
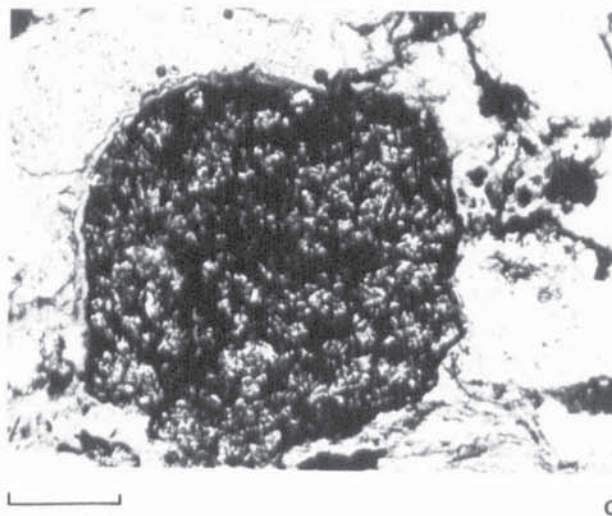
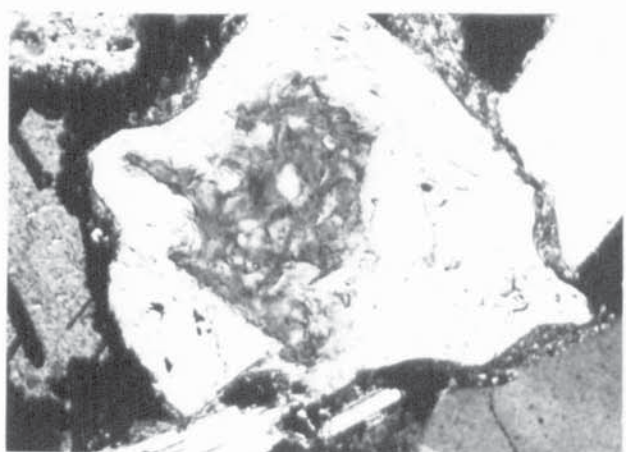
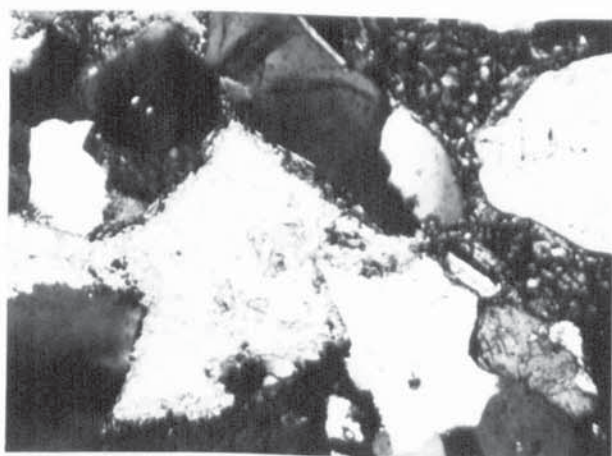


PLATE 3.3

- a) P8: Poikilotopic non-ferroan dolomite cement replaces and corrodes framework grains.  
Scale bar = 0.1mm
- b) P8: Etched dolomite crystals.  
Viewed under S.E.M.  
Scale bar = 20 $\mu$ m
- c) P8: Specular haematite grains with rounded margins indicating some degree of transport has occurred.  
Viewed under reflected light.  
Scale bar = 35 $\mu$ m
- d) P8: Embayed and altered skeletal haematite grain.  
Viewed under reflected light.  
Scale bar = 50 $\mu$ m
- e) P7: Tabular shaped haematite grain. May represent a pseudomorph after ilmenite.  
Viewed under reflected light.  
Scale bar = 50 $\mu$ m
- f) P5: Abundant pore filling diagenetic fine grained iron oxide (replacement of iron rich carbonates).  
Scale bar = 0.1mm

Plate 3.3

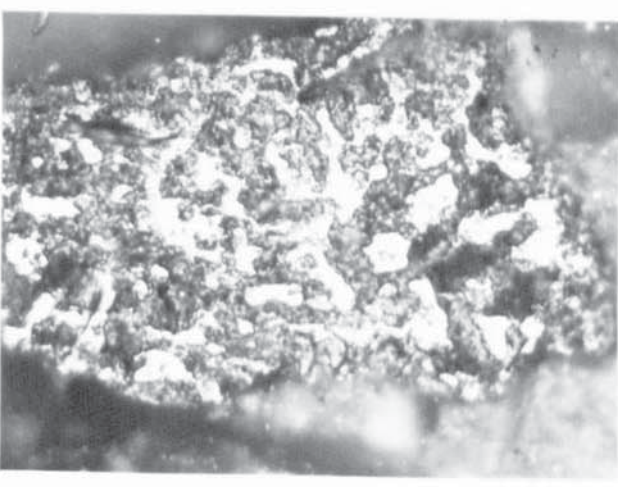
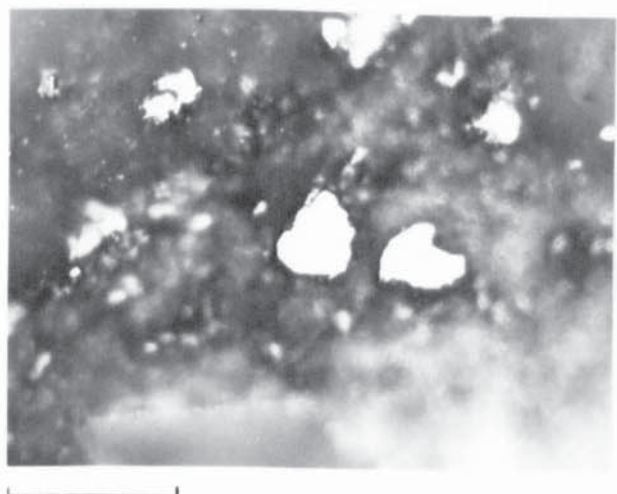
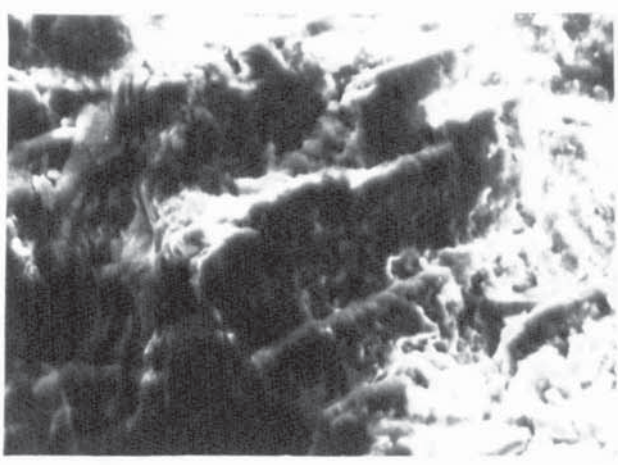
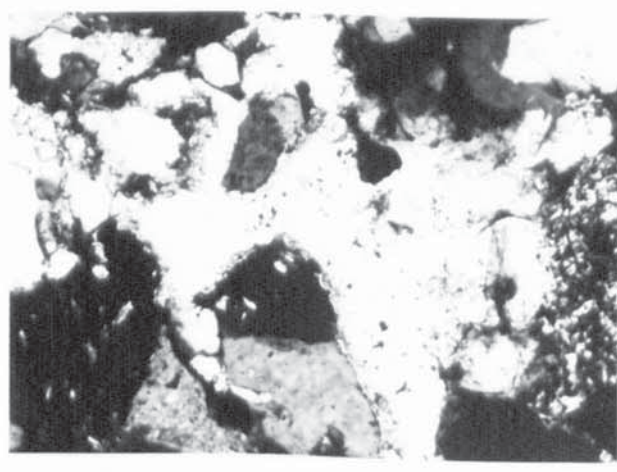


PLATE 4.1

View west-northwest of Saxonian run beds  
overlain by Lower Buntsandstein conglomerates.  
Thrust faulting has led to a repetition of the  
sequence. Torres de Albarracin section.

Plate 4.1

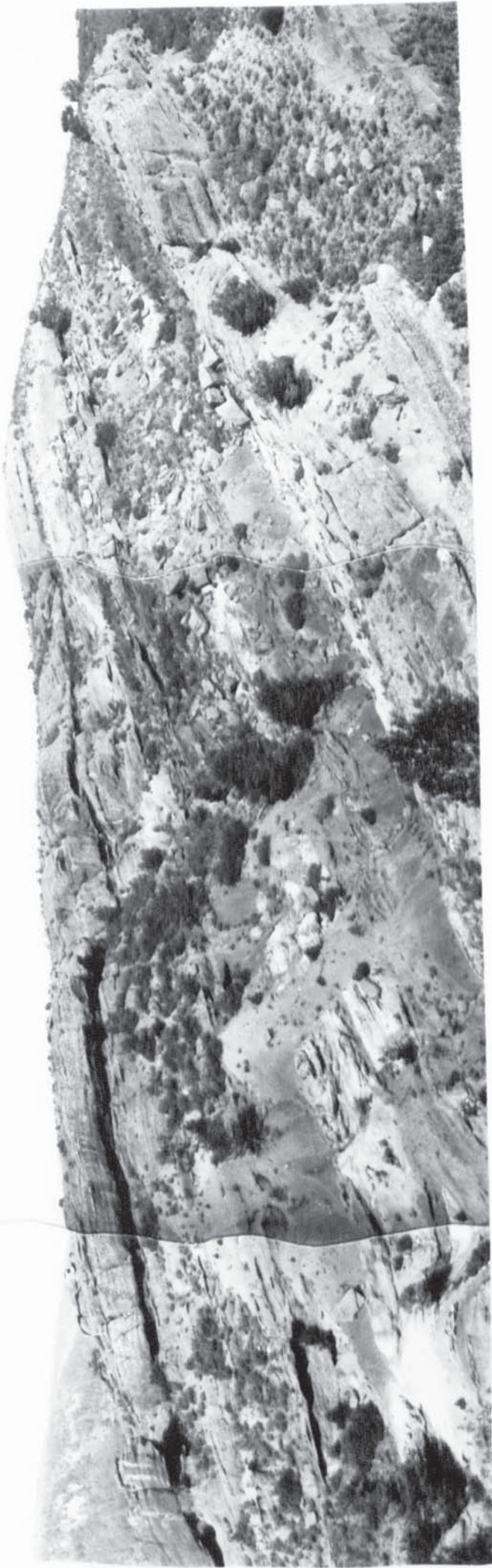
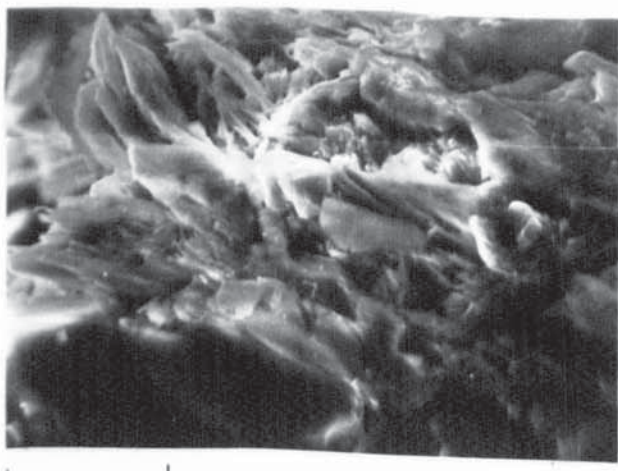
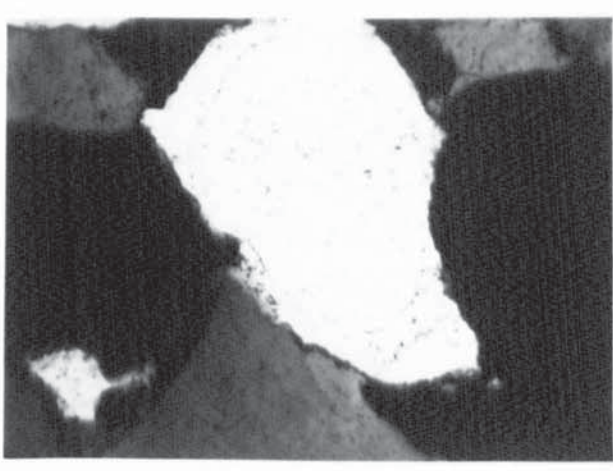


PLATE 4.2

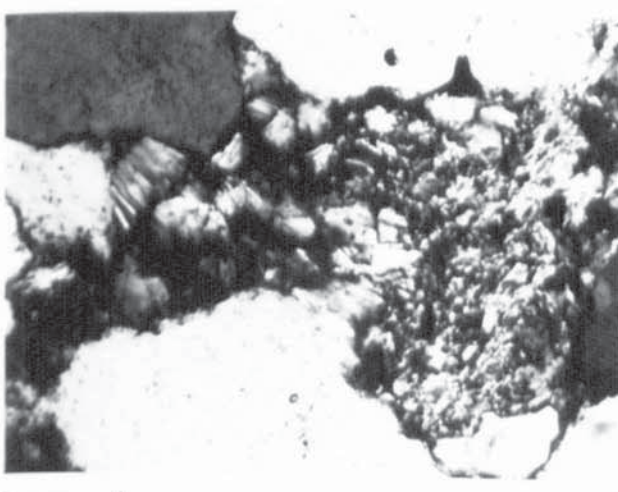
- a) MA115: Replacement of mica by authigenic illite.  
Viewed under S.E.M.  
Scale bar = 20 $\mu$ m
- b) MA112: Detrital quartz showing two phases of syntaxial authigenic overgrowths  
Scale bar = 0.1mm
- c) MA112: Pore filling authigenic kaolinite and grain replacing authigenic illite.  
Scale bar = 0.1mm
- d) MA116: Authigenic barite cement which post dates authigenic quartz.  
Scale bar = 0.2mm
- e) MA112: Embayed, detrital and authigenic quartz showing 'v' shaped notches and cemented by abundant iron oxide.  
Scale bar = 0.2mm
- f) MA116: Embayed detrital and authigenic quartz 'floating' in porefilling iron oxide cement. Note also moldic porosity (centre), due to dissolution of framework grain.  
Scale bar = 0.1mm



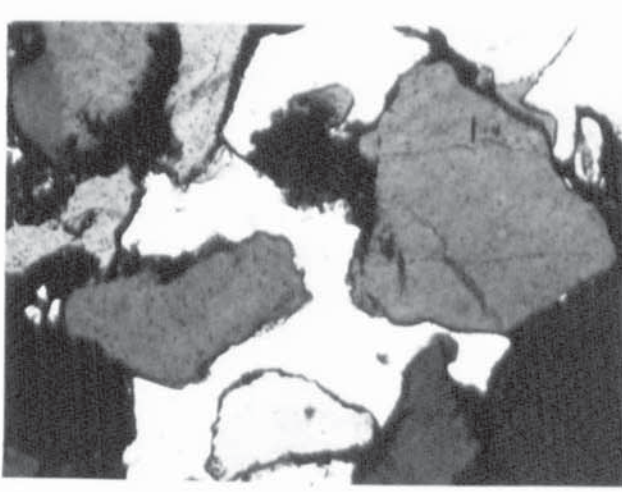
a



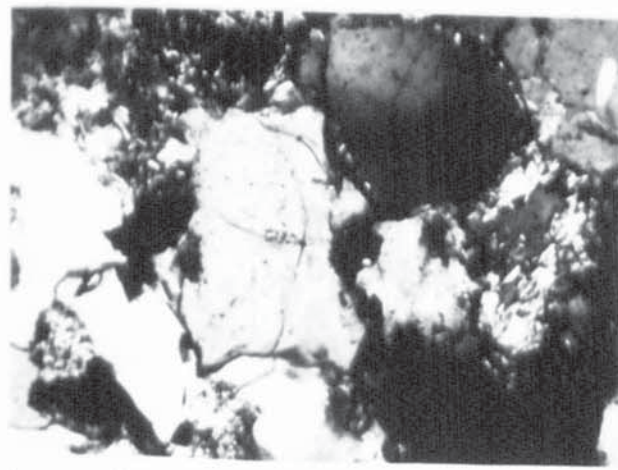
b



c



d

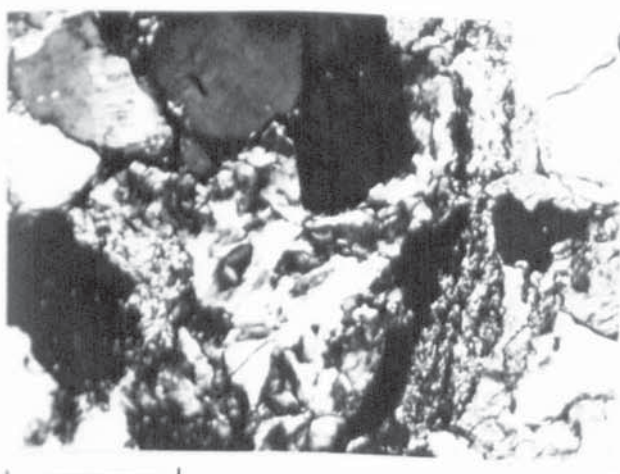


e

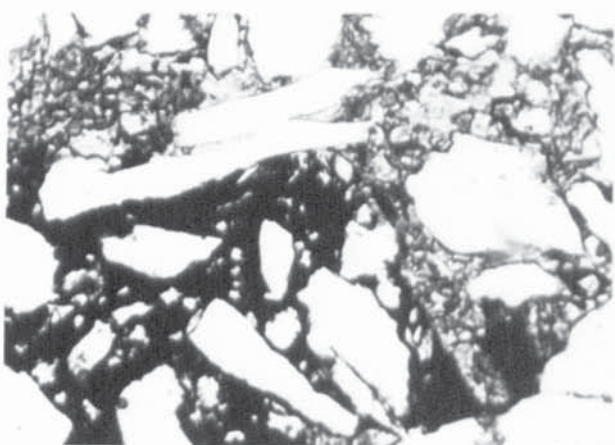


PLATE 4.3

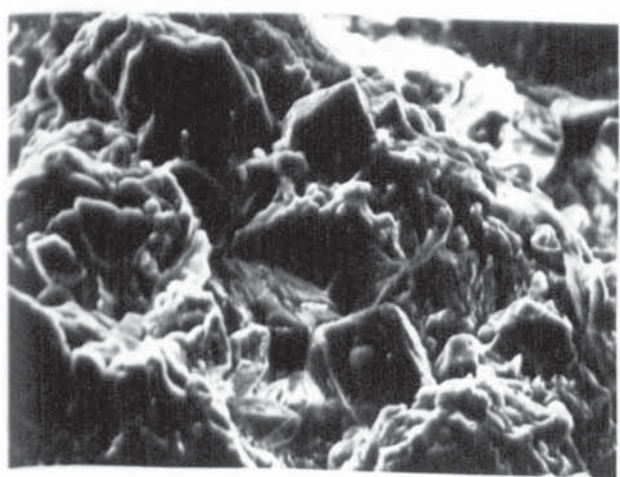
- a) PN3: Oversized pore filled with authigenic kaolinite.  
Scale bar = 0.2mm
- b) PN4: Aggressive, rhombic shaped patch of siderite cement surrounded by non-ferroan dolomite. Note the highly embayed and indented nature of the detrital grains.  
Scale bar = 0.2mm
- c) PN3: Non-ferroan dolomite rhombs cementing detrital grains.  
Viewed under S.E.M.  
Scale bar = 40 $\mu$ m
- d) PN3: Oversized pores and embayed quartz grains.  
Scale bar = 0.5mm
- e) TA2: Partial replacement of muscovite mica by authigenic kaolinite.  
Scale bar = 0.2mm
- f) TA4: 'V' shaped dissolution notches on surface of authigenic quartz.  
Viewed under S.E.M.  
Scale bar = 10 $\mu$ m



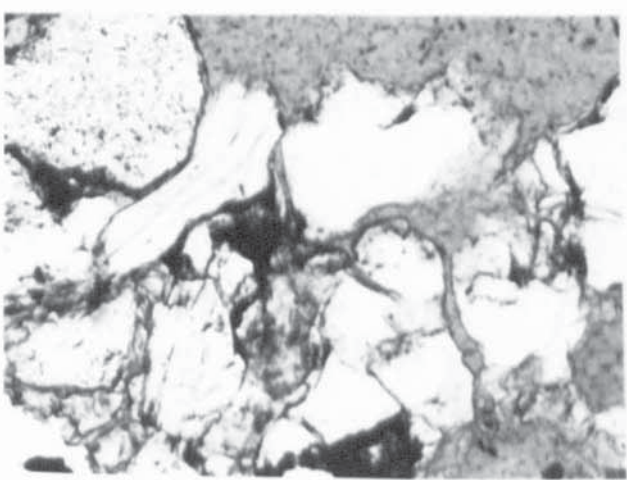
a



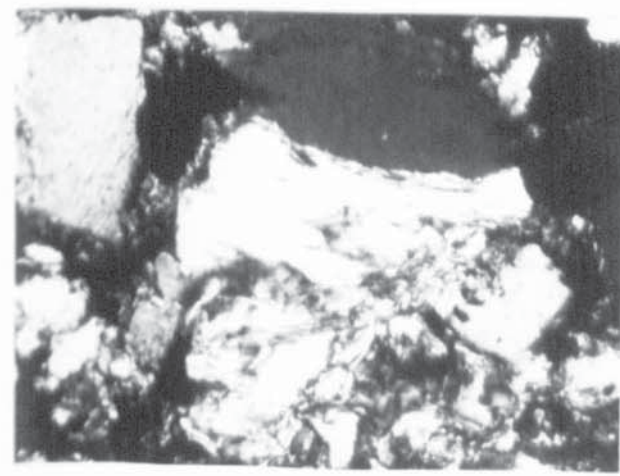
b



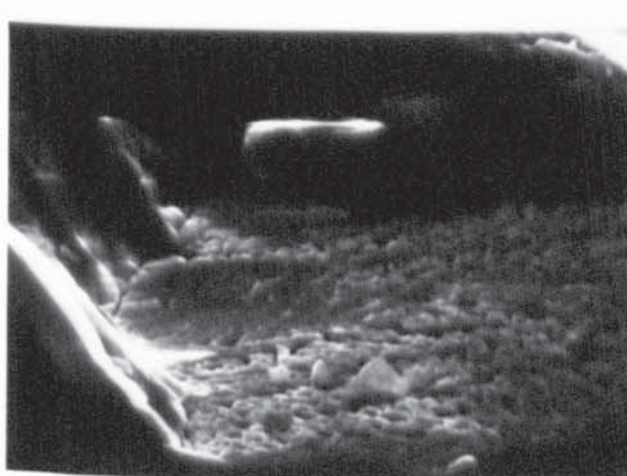
c



d



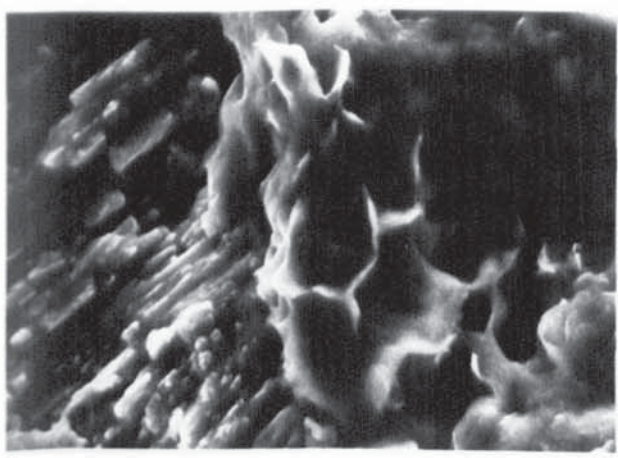
e



f

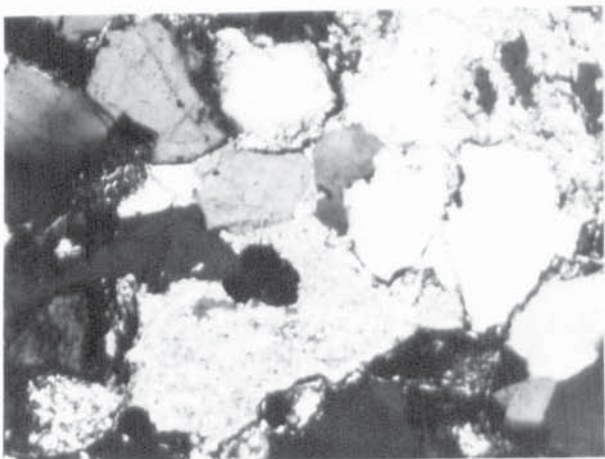
PLATE 4.4

- a) TA8: Authigenic clay (right) demonstrating 'honeycomb' texture. This is typical of mixed layer illite/smectite clays. Etched feldspar (left).  
Viewed under S.E.M.  
Scale bar = 10µm
- b) TA2: Aggressive, poikilotopic non-ferroan dolomite cement which corrodes both detrital and authigenic quartz.  
Scale bar = 0.2mm
- c) TA1: Framework grains cemented by siderite. Note 'V' shaped indentations into detrital and authigenic quartz.  
Scale bar = 0.2mm
- d) TA1: Partial replacement of siderite cement by fine grained iron oxide.  
Viewed under S.E.M.  
Scale bar = 10µm
- e) MA114: Detrital haematite grain also containing ilmenite (darker area).  
Viewed under reflected light.  
Scale bar = 50µm
- f) MA114: Detrital haematite grain showing alteration to fine grained iron oxide and titanium oxide (bright areas).  
Viewed under reflected light.  
Scale bar = 50µm



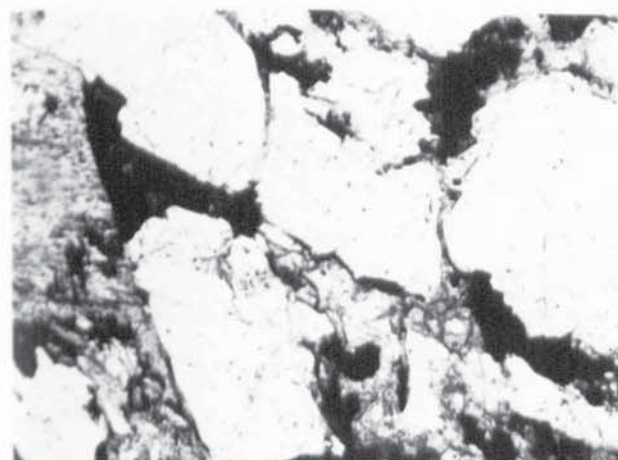
[ ]

a



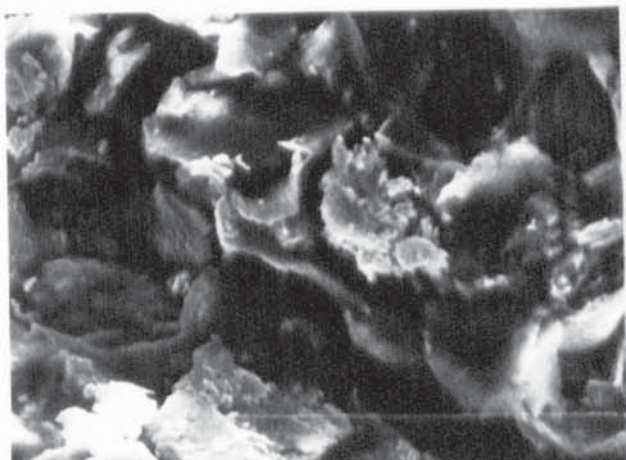
[ ]

b



[ ]

c



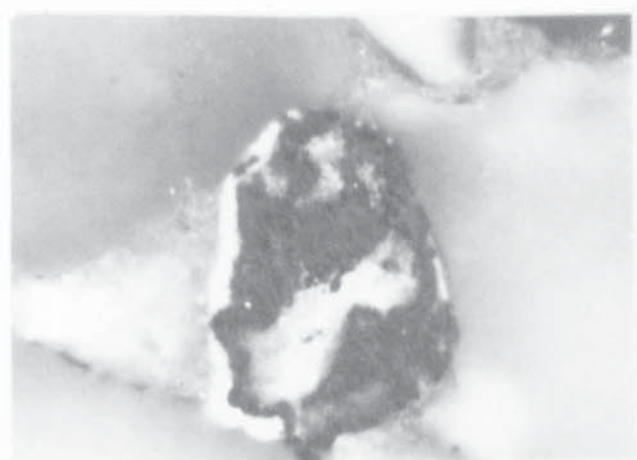
[ ]

d



[ ]

e

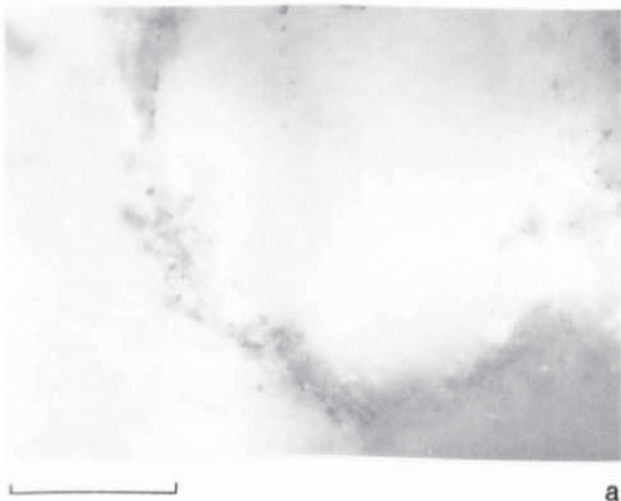


[ ]

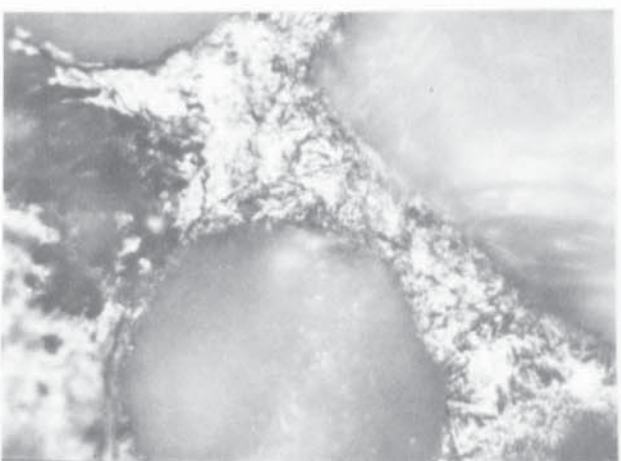
f

PLATE 4.5

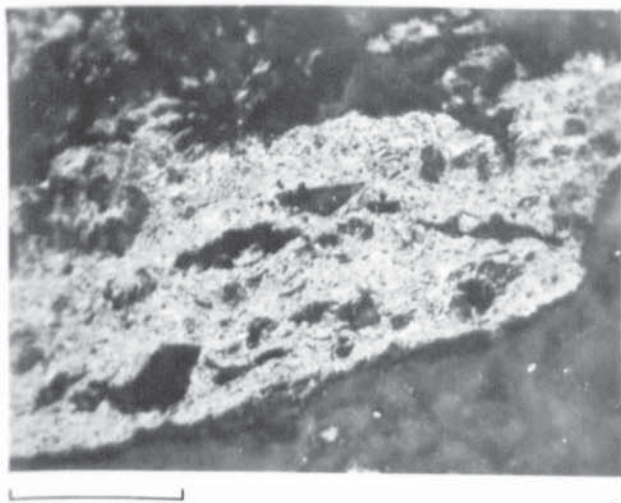
- a) MA115: Grain rimming fine grained iron oxide associated with detrital clay.  
Viewed under reflected light.  
Scale bar = 50 $\mu$ m
  
- b) MA112: Pore filling microcrystalline haematite.  
Viewed under reflected light.  
Scale bar = 50 $\mu$ m
  
- c) MA112: Rock fragment showing almost total replacement by microcrystalline haematite.  
Viewed under reflected light.  
Scale bar = 50 $\mu$ m
  
- d) MA116: Euhedral, acicular crystals of authigenic titanium oxide.  
Viewed under reflected light.  
Scale bar = 50 $\mu$ m
  
- e) PN3: Pore filling siderite cement which has been partially replaced by fine grained iron oxide.  
Scale bar = 0.1mm
  
- f) MA116: Pore filling haematite cement.  
Viewed under reflected light.  
Scale bar = 50 $\mu$ m



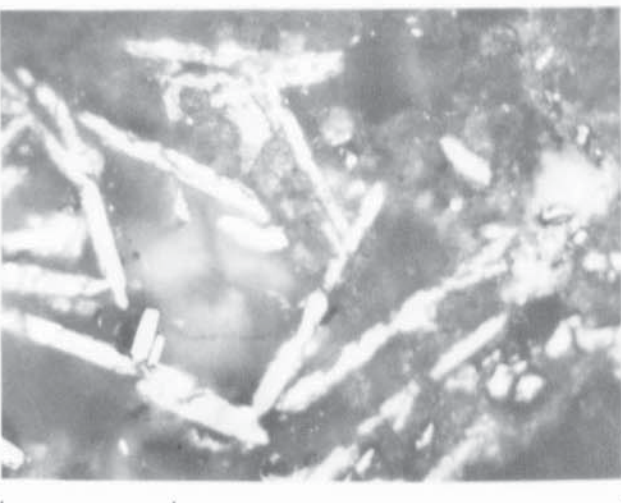
a



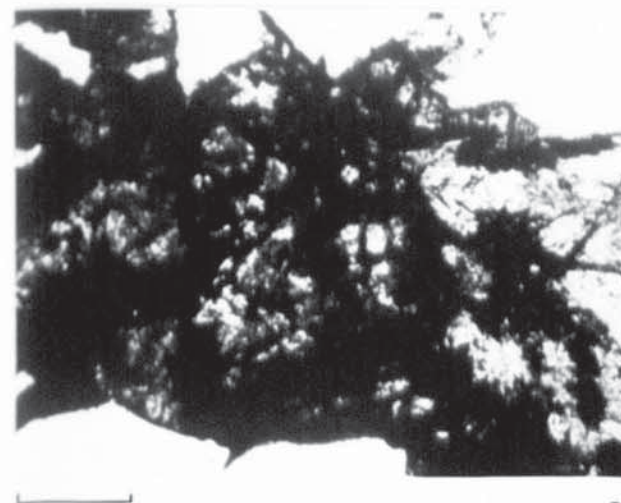
b



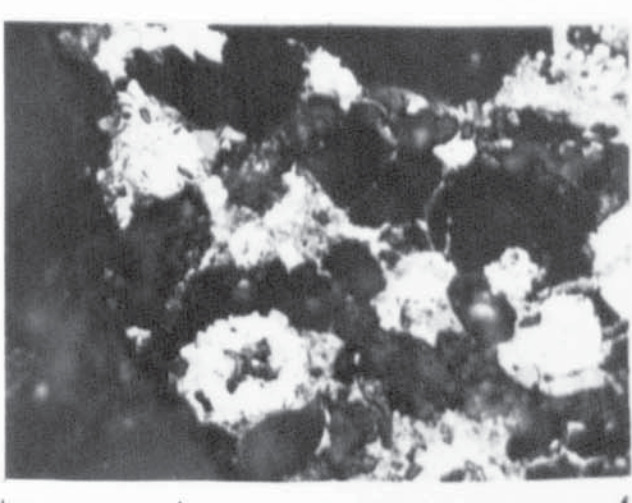
c



d



e

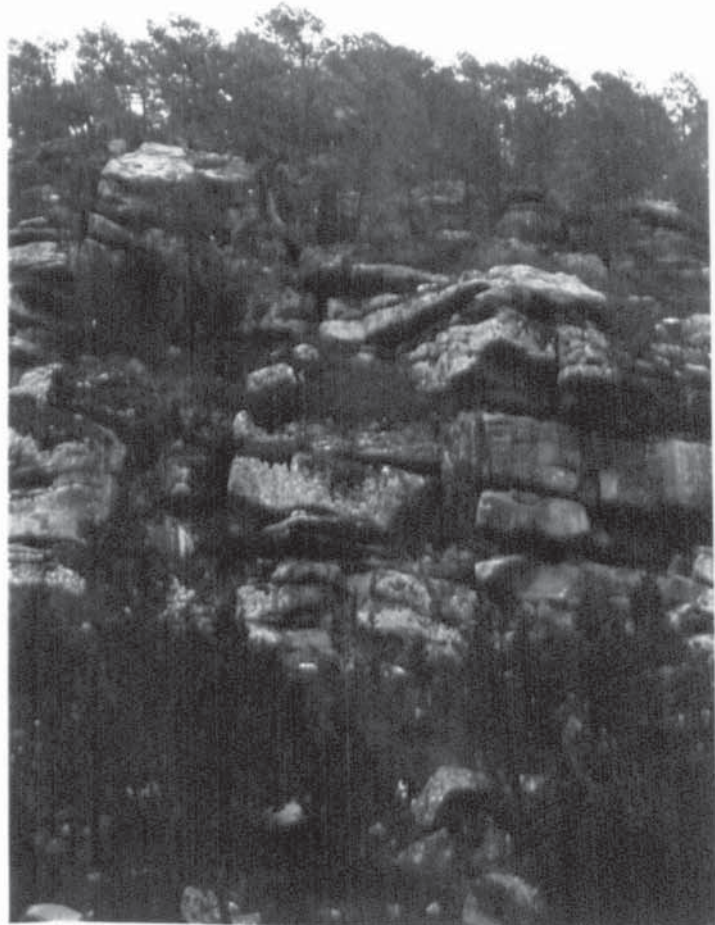


f

PLATE 5.1

- a) View looking southwest of Lower Triassic sediments from the Hoz del Gallo section, near Molina de Aragon, Central Spain.
- b) View looking west-southwest at Sandstones of the Rillo de Gallo Sandstone unit from the Rillo de Gallo section, near Molina de Aragon, Central Spain.

**Plate 5.1**



**a**



**b**

PLATE 5.2

- a) MA52: Severely etched feldspar grain showing creation of moldic porosity.  
Scale bar = 0.1mm
- b) MA41: Polygranular rock fragments of sedimentary origin, composed predominantly, of quartz grains with abundant clay matrix. Probably derived from the underlying Permian deposits.
- c) MA13: Igneous rock fragment (centre) demonstrating graphic texture. Quartz with authigenic overgrowth(Q).  
Scale bar = 0.1mm
- d) MA48: Pore ocellating authigenic quartz cement.  
Scale bar = 0.5mm
- e) MA41: Authigenic, non-syntaxial potassium feldspar. (Note that it predates authigenic quartz).  
Scale bar = 0.1mm
- f) MA6: Pore lining (high birefringent) illite and pore filling authigenic kaolinite.  
Scale bar = 0.1mm

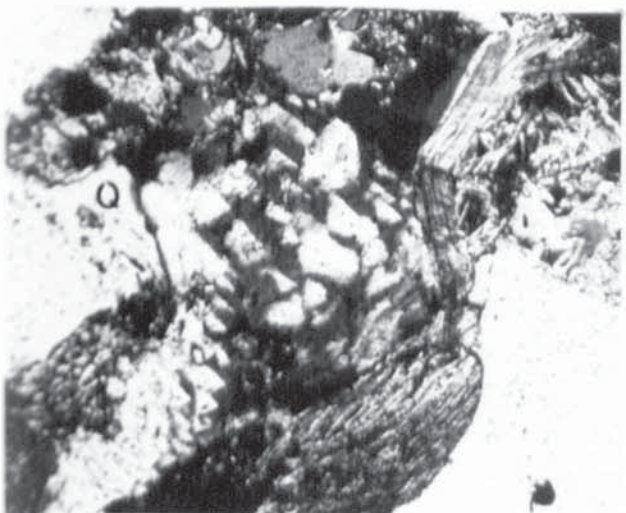
**Plate 5.2**



a



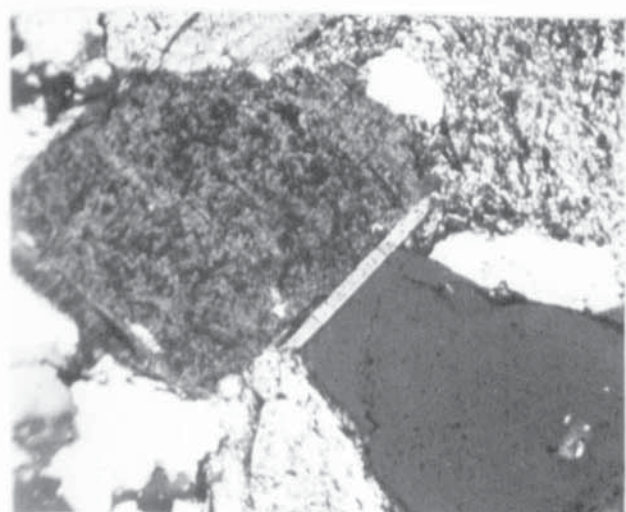
b



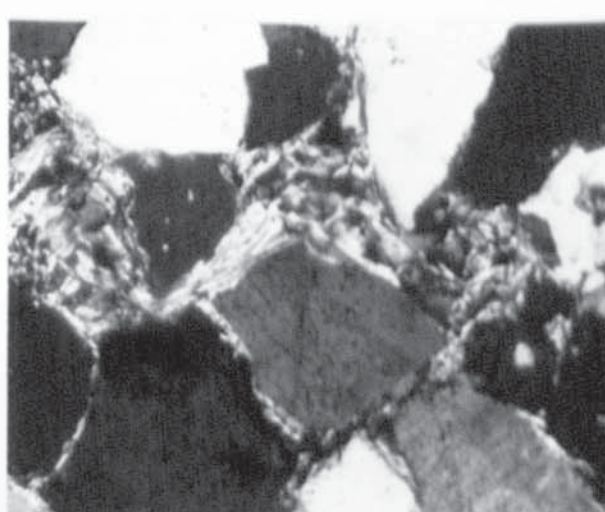
c



d



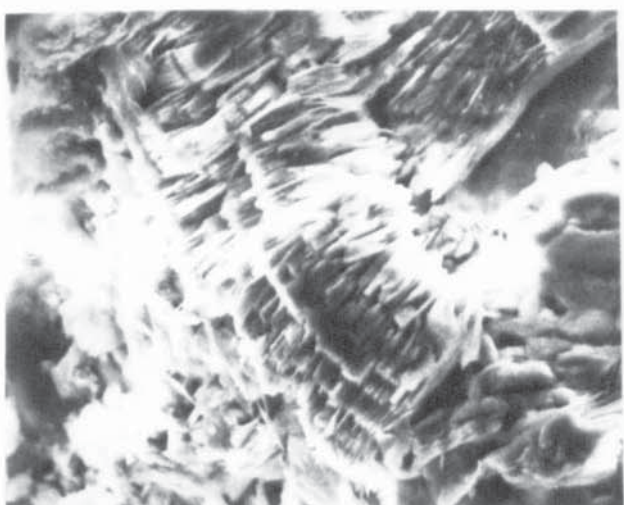
e



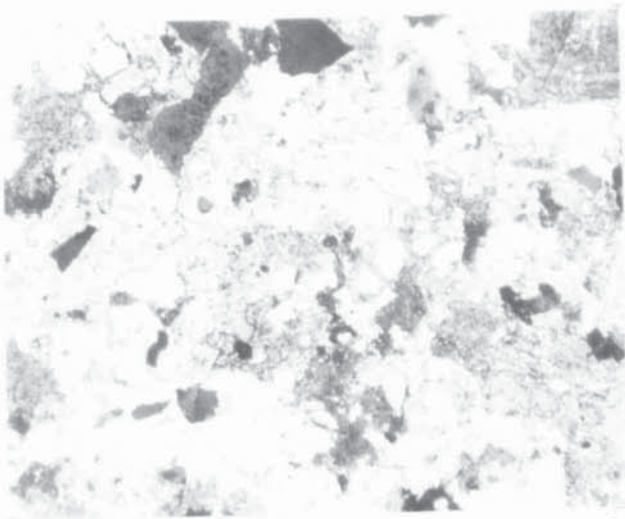
f

PLATE 5.3

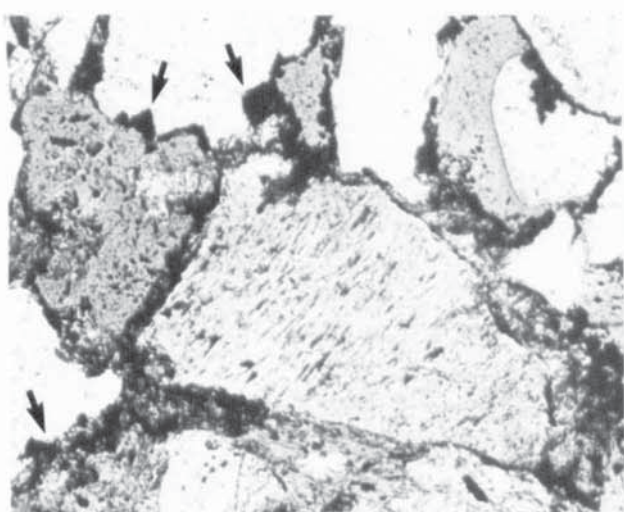
- a) MA8: Coarse 'Vermiform' booklet of authigenic kaolinite.  
Viewed under S.E.M.  
Scale bar = 20 $\mu$ m
  
- b) MA57: Aggressive, poikilotopic, non-ferroan dolomite cement. Note the highly embayed nature of the detrital grains.  
Scale bar = 0.5mm
  
- c) MA41: Small 'V' shaped notches (arrowed) etched into quartz grains. Note thick pore lining of authigenic iron oxide.  
Scale bar = 0.1mm
  
- d) MA44: Oversized, rhomb shaped secondary pores.  
Scale bar = 0.5mm
  
- e) MA11: Skeletal, rounder detrital haematite grain.  
Viewed under reflected light.  
Scale bar = 50 $\mu$ m
  
- f) MA51: Tabular grain of amorphous titanium oxide (leucoxene) after ilmenite.  
View under reflected light.  
Scale bar = 0.1mm



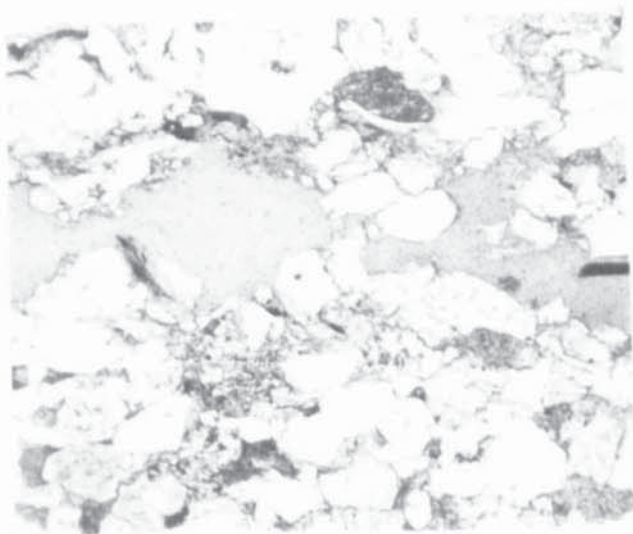
a



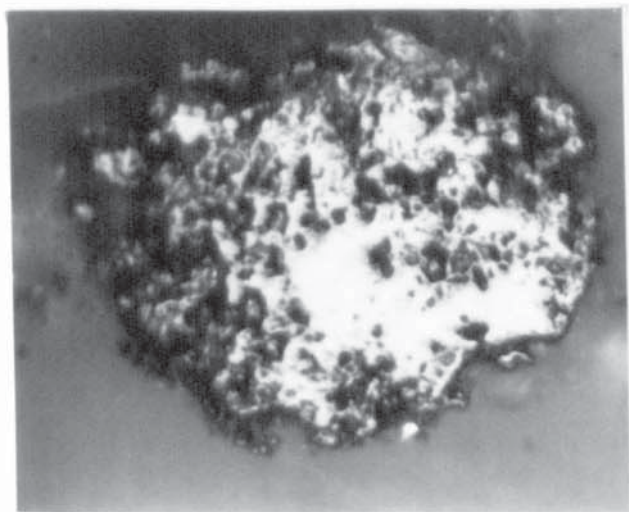
b



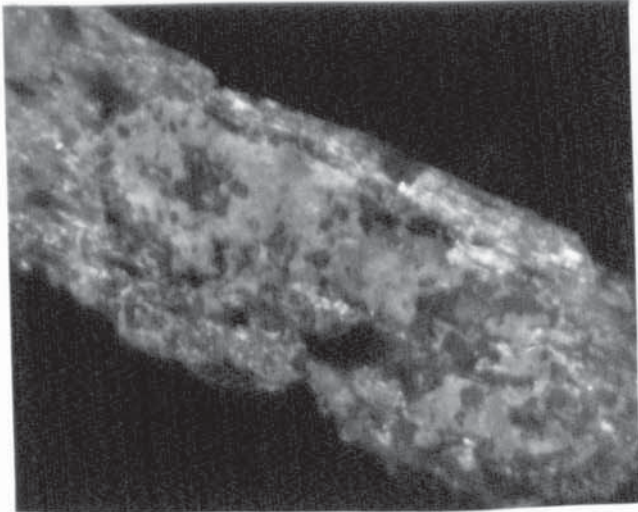
c



d



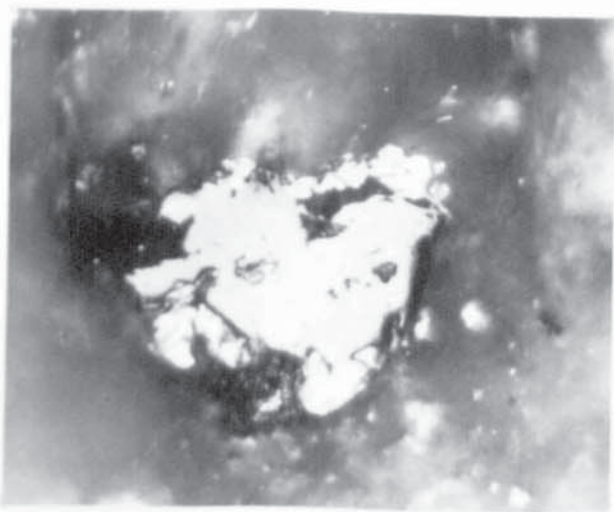
e



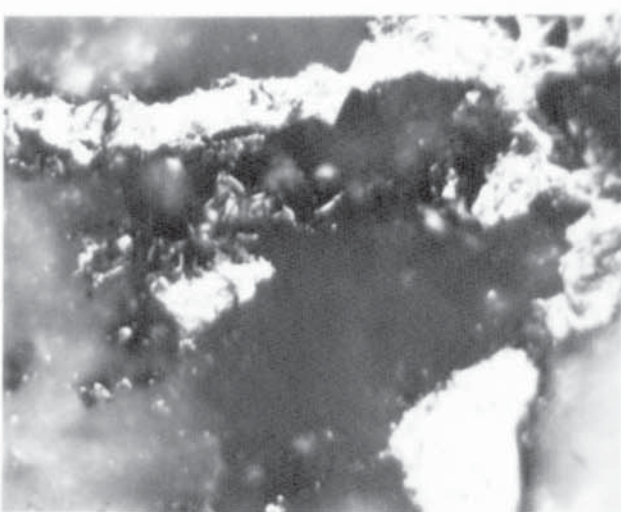
f

PLATE 5.4

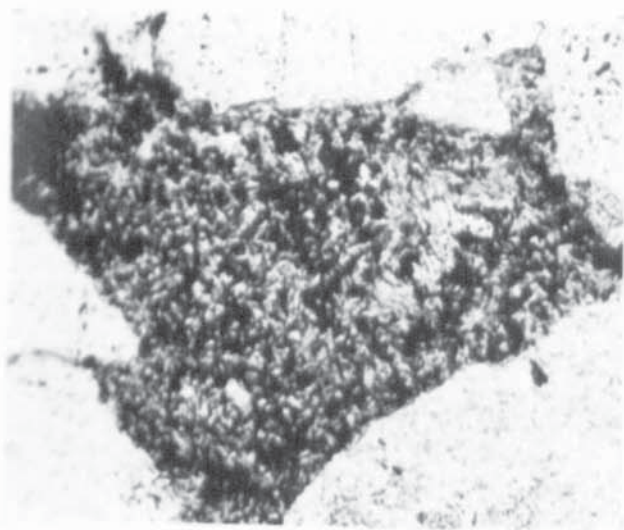
- a) MA10: detrital specularite grain with titanium oxide at the margins.  
Viewed under reflected light.  
Scale bar = 50 $\mu$ m
  
- b) MA10: Grain rimming authigenic microcrystalline haematite.  
Viewed under reflected light.  
Scale bar = 50 $\mu$ m.
  
- c) MA8: Pore filling, fine grained iron oxide and kaolinite.  
Scale bar = 0.1mm
  
- d) MA10: Pore filling microcrystalline haematite associated with pore filling clays? Note etched silicate grains.  
Viewed under reflected light.  
Scale bar = 50 $\mu$ m
  
- e) MA2: Abundant pore filling goethite viewed under reflected light.  
Scale bar = 0.1mm
  
- f) MA2: Unusual 'nobbly' habit of authigenic goethite.  
Viewed under S.E.M.  
Scale bar = 4 $\mu$ m



a



b



c



d



e



f

PLATE 6.1

- a) View southwest showing tabular cross-bedding underlain by planar bedding in the Rio Arandilla Sandstones of the Rillo de Gallo section, near Molina de Aragon, Central Spain.
- b) View west-southwest through a lateral accretion belt demonstrating epsilon cross-bedding. Rio Arandilla Sandstones unit, Rio Arandilla section, near Molina de Aragon, Central Spain.

**Plate 6.1**



**a**

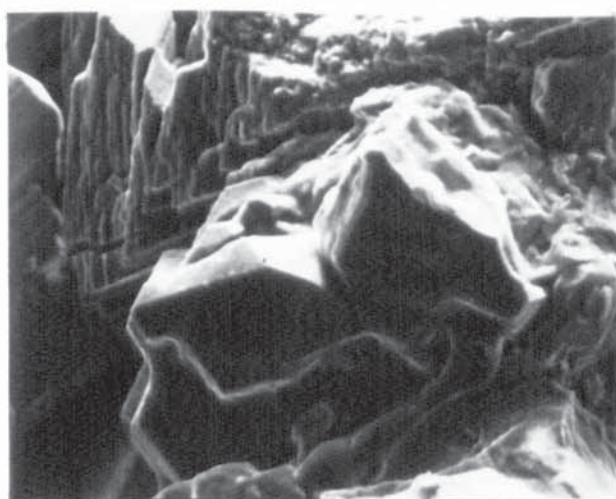


**b**

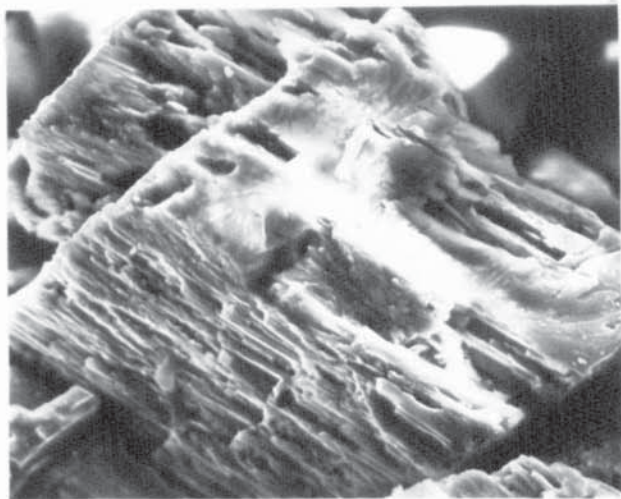
PLATE 6.2

- a) MA62: Authigenic quartz overgrowth on detrital grain (foreground).  
Authigenic potassium feldspar background.  
Viewed under S.E.M.  
Scale bar = 40µm
- b) MA72: Etched, euhedral authigenic potassium feldspar.  
Viewed under S.E.M.  
Scale bar = 20µm
- c) MA67: Abundant pore filling and replacement clays.  
Scale bar = 0.5mm
- d) MA62: Neomorphic kaolinite splayed cleavage muscovite mica.  
Scale bar = 0.1mm
- e) RA2: Poikilotopic non-ferroan dolomite cement.  
Scale bar = 0.5mm
- f) MA73: Euhedral rhombs of authigenic dolomite cement.  
Viewed under S.E.M.  
Scale bar = 10µm

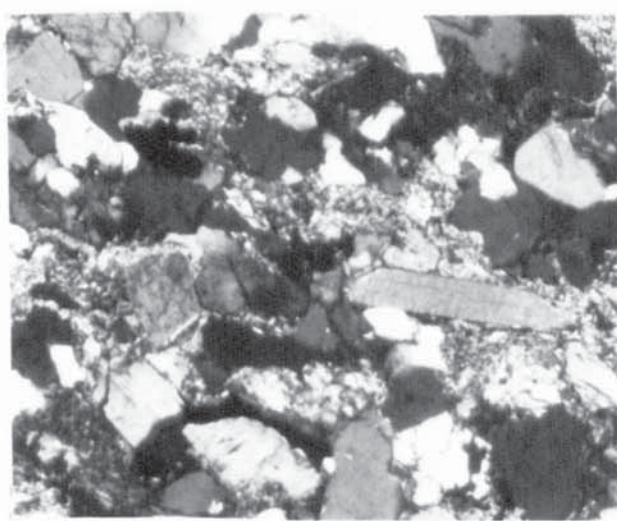
**Plate 6.2**



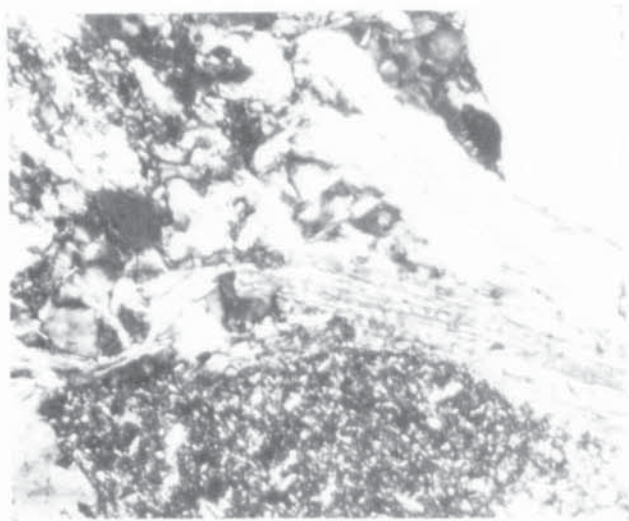
a



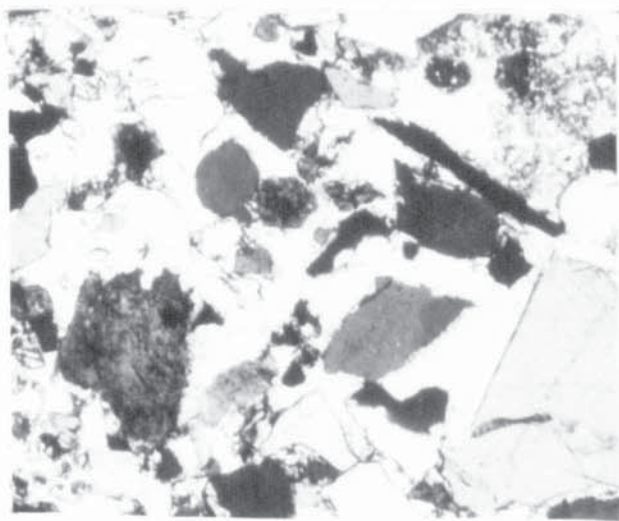
b



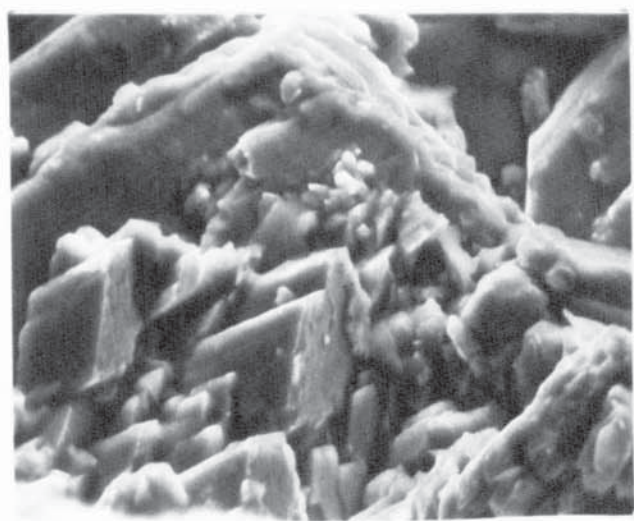
c



d



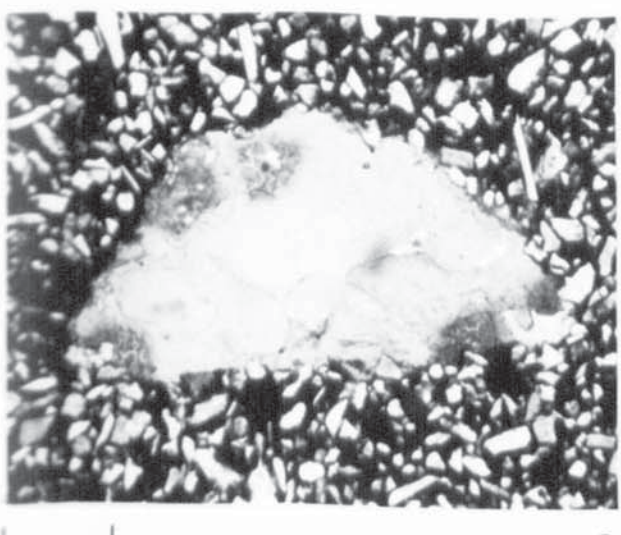
e



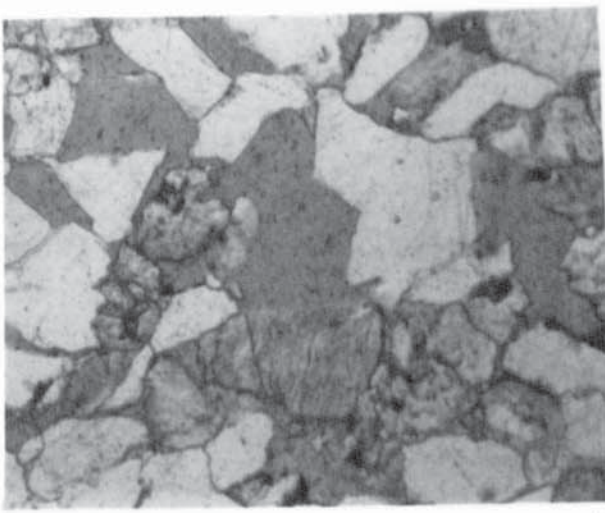
f

PLATE 6:3

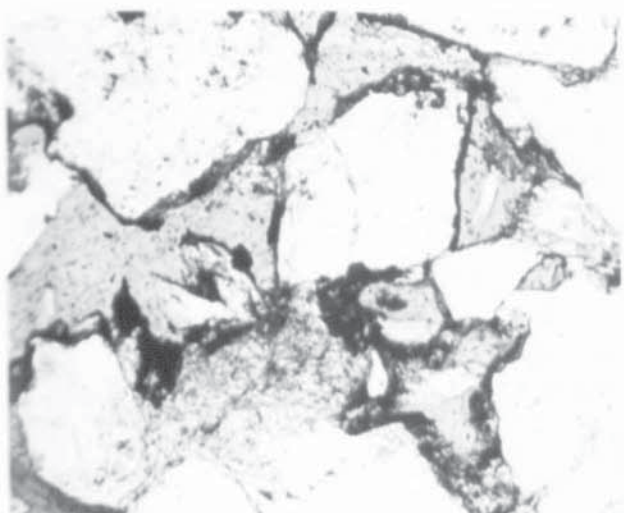
- a) MA89: Euhedral non-ferroan dolomite nodule with ferroan calcite rhombs at margin (darker areas). Note also, iron oxide and clay rich matrix in which detrital grains appear to 'float'.  
Scale bar = 0.5mm
- b) MA64: Oversized pore due to framework grain and/or cement dissolution.  
Scale bar = 0.1mm
- c) MA63: Secondary pore lined with iron oxide which post dates authigenic quartz.  
Scale bar = 0.1mm
- d) MA71: Rounded detrital opaque grain.  
Scale bar = 0.1mm
- e) MA91: Embayed, skeletal detrital specularite grains.  
Viewed in reflected light.  
Scale bar = 40µm
- f) MA91: Detrital titanium oxide grain partially replaced by haematite (dark areas).  
Viewed in reflected light.  
Scale bar = 50µm



a



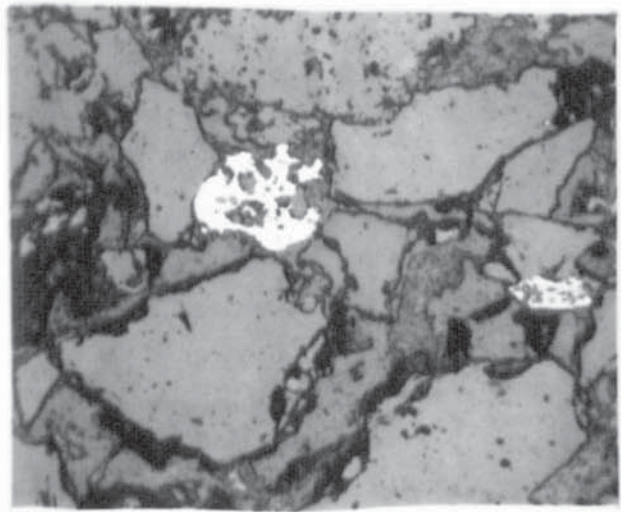
b



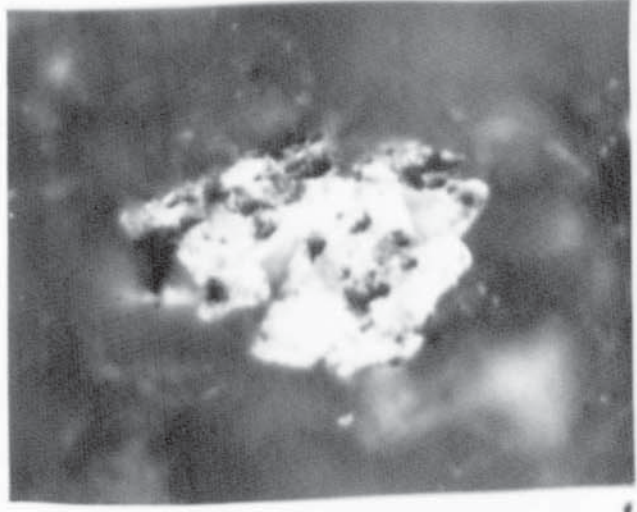
c



d



e



f

PLATE 6.4

- a) MA67: Tabular grains of detrital titanium oxide.  
Scale bar = 0.1mm
  
- b) MA67: Same view as 6.5a but viewed in reflected light. This shows the typical corroded appearance of detrital titanium oxides.  
Scale bar = 0.1mm
  
- c) RA6: Authigenic microcrystalline haematite, perhaps occurring as replacement of cleaved silicate mineral.  
Viewed in reflected light.  
Scale bar = 20 $\mu$ m
  
- d) MA93: Fine grained iron oxide associated with clays.  
Viewed under S.E.M.
  
- e) RA9: Severely embayed framework grains 'floating' in iron oxide and clay rich matrix.  
Scale bar = 0.1mm
  
- f) MA84: Fine grained pore filling iron oxide and titanium oxide.  
Viewed in reflected light.  
Scale bar = 0.1mm

**Plate 6.4**

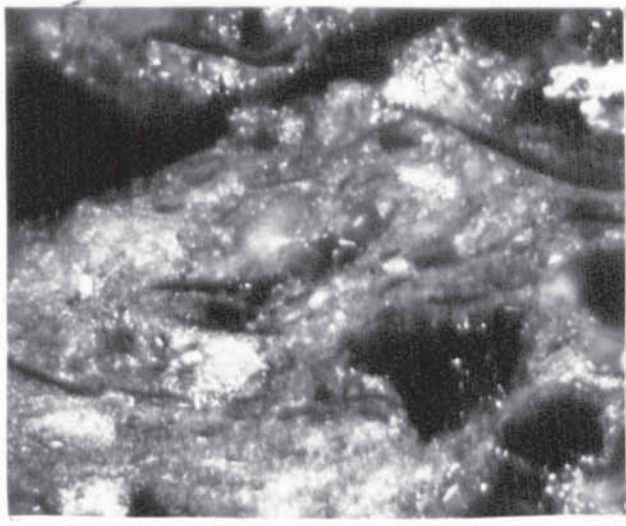
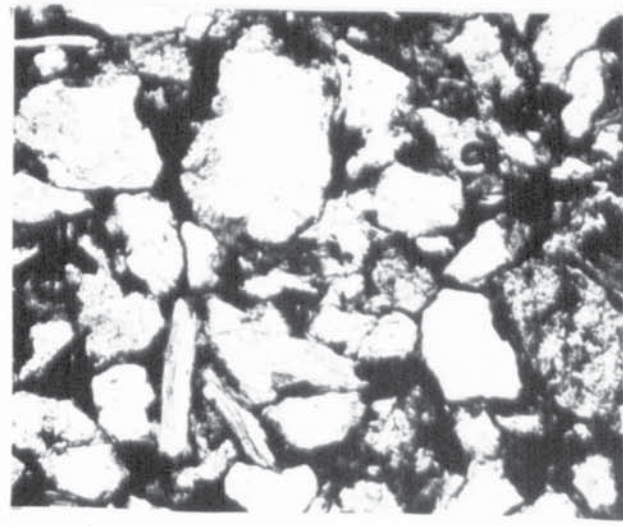
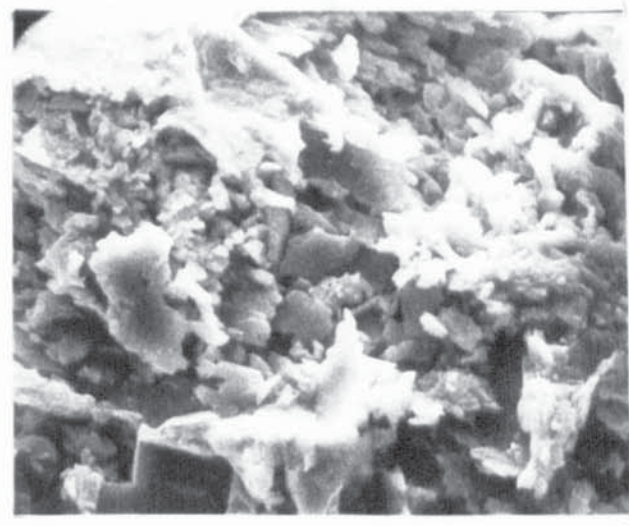
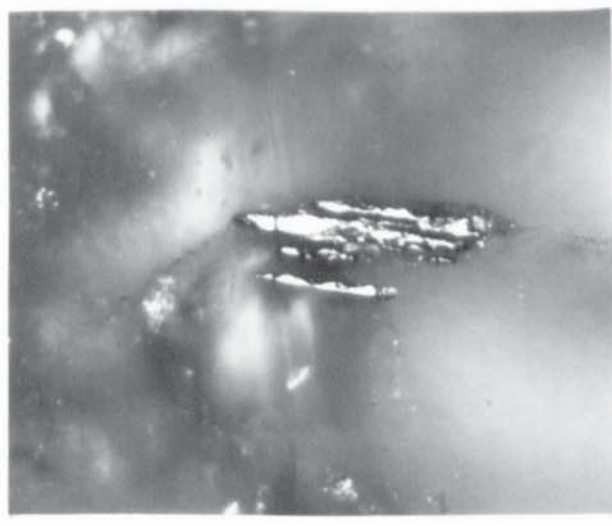
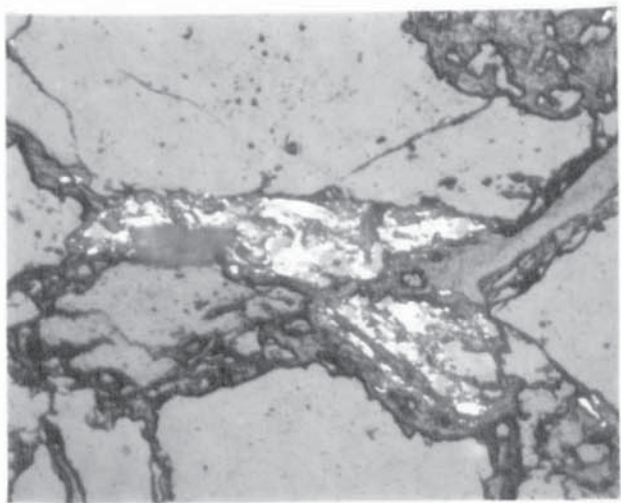
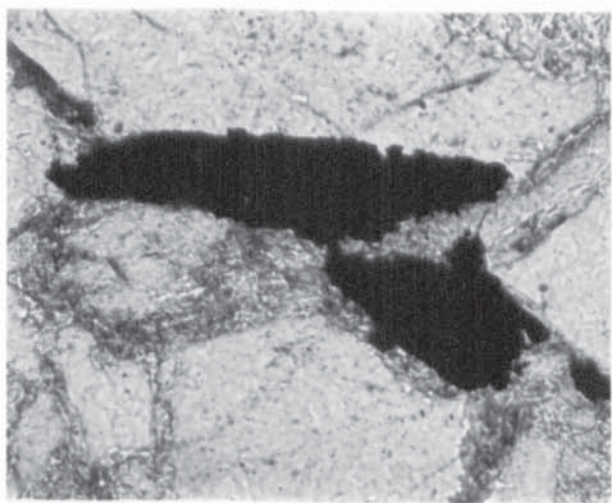


PLATE 7.1

- a) Upper part of the "Dolomites, marls and caliches of Royuela", Muschelkalk facies, exposed in road cutting. Castellar de la Muella, Sierra de Caldereros.
- b) Locality of samples MA104-MA106, interbedded marls and dolomites. Royuela cap, Muschelkalk facies, Rillo de Gallo section. Near Molina de Aragon, Central Spain.
- c) General view northwest of the Keuper of Teroleja. Units exposed in this cliff section are: Teroleja mudstones (lower part), Teroleja Gypsum and mudstones, Teroleja gypsum and marls (light coloured, blocky horizon), and the Imon dolomite formation (upper part), from which samples T1-4 were taken.

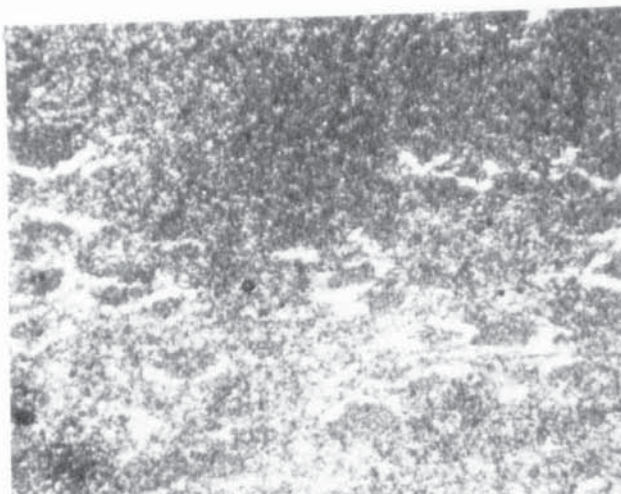
**Plate 7.1**



PLATE 7.2

- a) CM1: Ellipsoid features (compacted ooids?) in microcrystalline dolomite.  
Scale bar = 0.5mm
- b) CM3: Veinlet of non-ferroan dolomite and fibrous gypsum cutting through microcrystalline non-ferroan dolomite. Note also curved outline of shelly fossil (dark area).  
Scale bar = 0.1mm
- c) CM3: Euhedral rhombic shaped crystals of non-ferroan dolomite.  
Viewed under S.E.M.  
Scale bar = 4 $\mu$ m
- d) MA96: Coarsely crystalline veinlet of non-ferroan dolomite cutting through finely crystalline non-ferroan dolomite rich in organic matter.  
Scale bar = 0.5mm
- e) MA96: Recrystallised foram? in microcrystalline slightly ferroan dolomite.  
Scale bar = 0.5mm
- f) MA101: Irregular calcite veinlet cutting through microcrystalline non-ferroan dolomite. Note that the veinlet is lined with fine grained iron oxide.  
Scale bar = 0.5mm

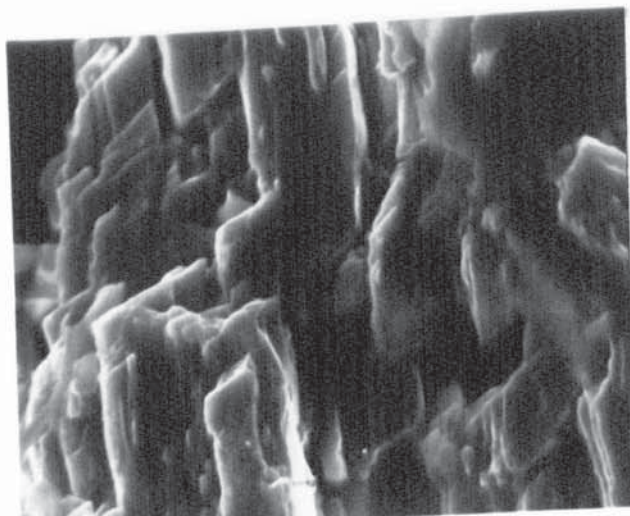
**Plate 7.2**



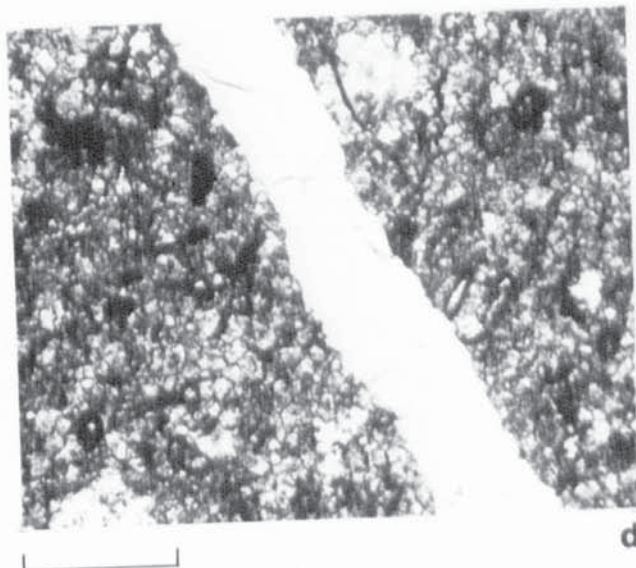
a



b



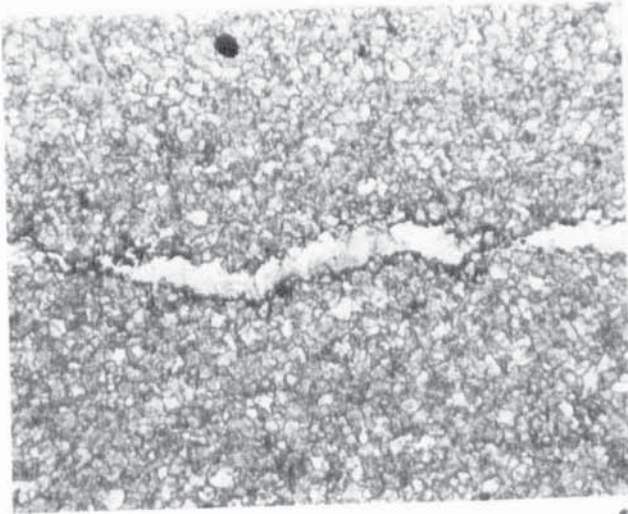
c



d



e

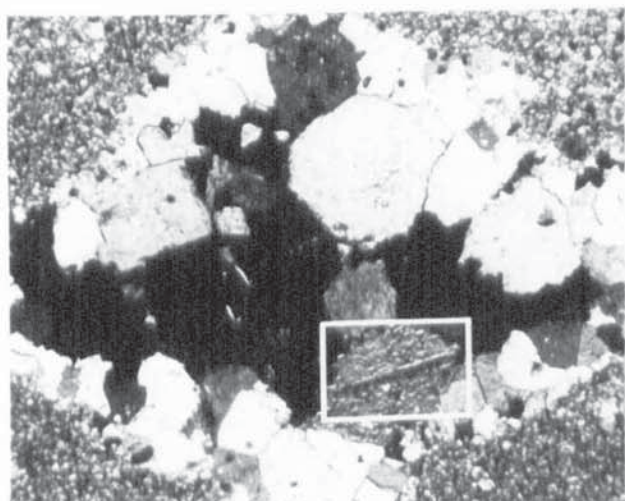


f

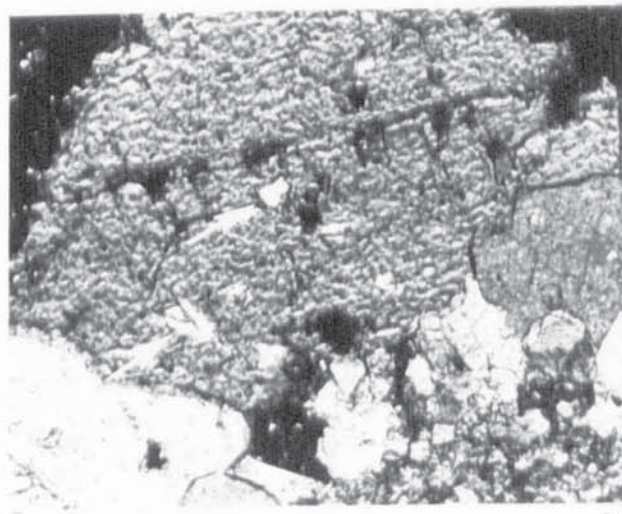
PLATE 7.3

- a) MA105: Lozenge shaped patch of coarse grained non-ferroan dolomite.  
Scale bar = 0.5mm
- b) MA105: Enlargement of part of 7.3a.  
Dolomite crystal contains relict anhydrite.  
Scale bar = 0.1mm
- c) MA97: Rhombs of coarsely crystalline dolomite non-ferroan at margins, ferroan in centre. In microcrystalline non-ferroan dolomite matrix.  
Scale bar 0.1mm
- d) MQ7: Euhedral overgrowths of authigenic feldspar.  
Scale bar = 0.1mm
- e) MQ4: Microcrystalline dolomite showing organic rich algal laminations?  
Scale bar = 0.5mm
- f) MQ8: Organic pellets in microcrystalline non-ferroan dolomite.  
Scale bar = 0.1mm

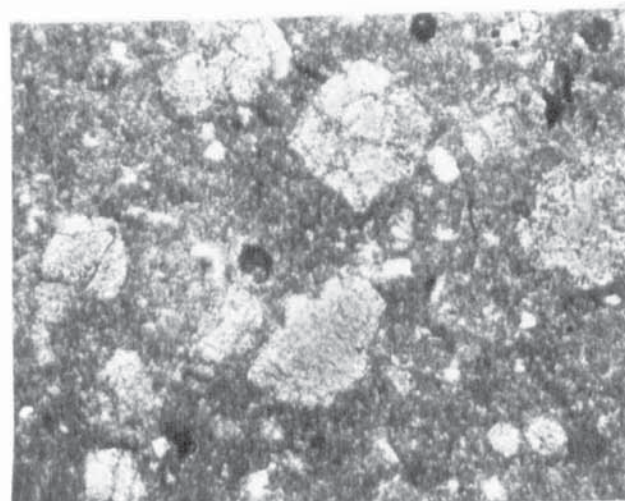
**Plate 7.3**



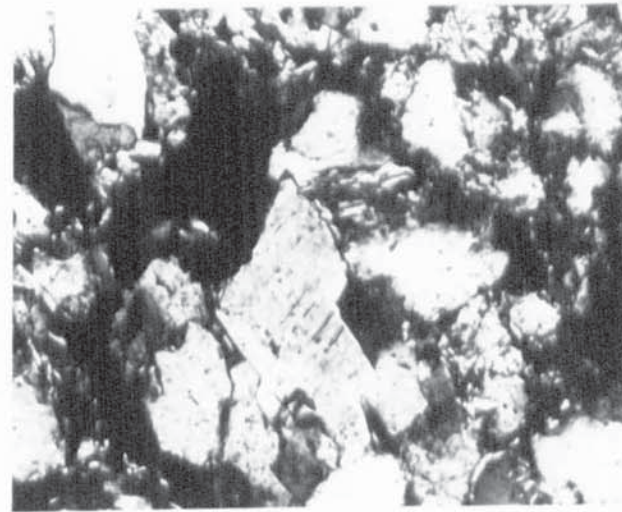
a



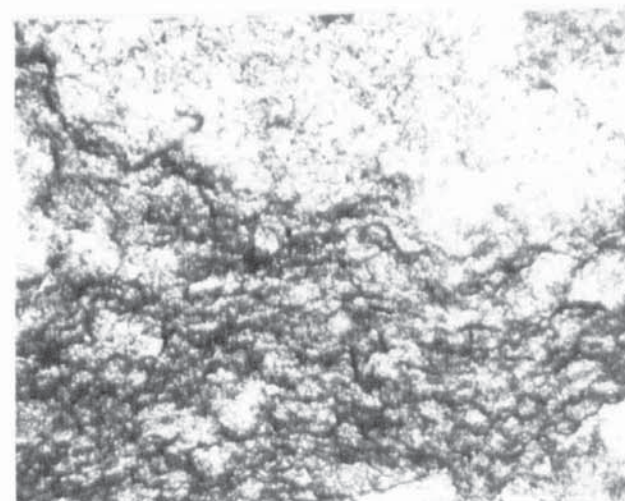
b



c



d



e



f

PLATE 7.4

- a) MQ8: Cross section through recrystallized chambered microfossil in non-ferroan microcrystalline dolomite.  
Scale bar = 0.5mm
- b) MQ8: Part of large vug partially infilled with coarse grained non-ferroan dolomite. Note rhombic shaped voids lined with fine grained iron oxide at margins.  
Scale bar = 0.5mm
- c) T1: Fine, organic rich laminations in microcrystalline non-ferroan dolomite. Small lensoid shapes patches of slightly coarse grained non-ferroan dolomite.  
Scale bar = 0.5mm
- d) T2: Crescent shapes void lined with small ferroan calcite crystals.  
Scale bar = 0.5mm
- e) T1: Lensoid shaped patch of low birefringent barite, almost totally replaced by coarse grained non-ferroan dolomite.  
Scale bar = 0.5mm
- f) T4: Dolomite breccia cemented non-ferroan dolomite.  
Scale bar = 0.1mm

**Plate 7.4**

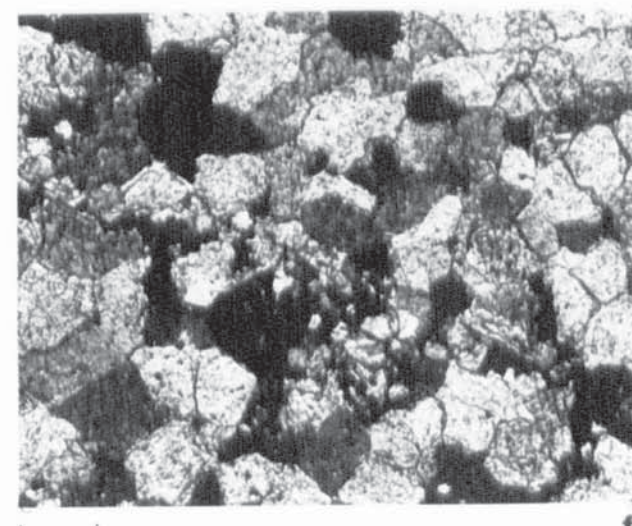
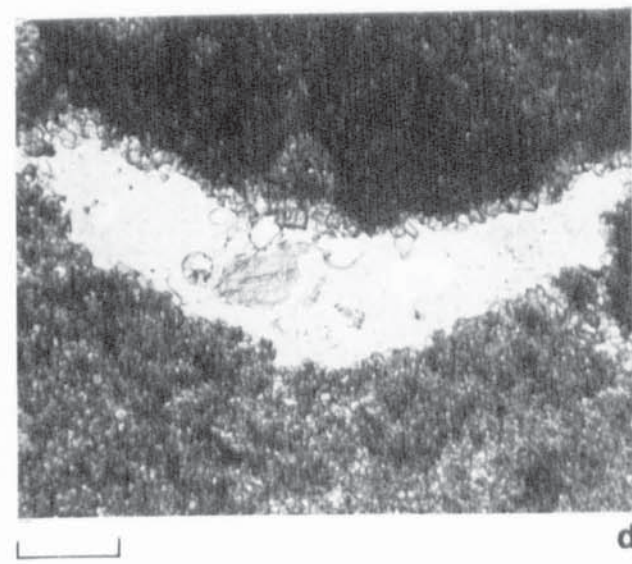
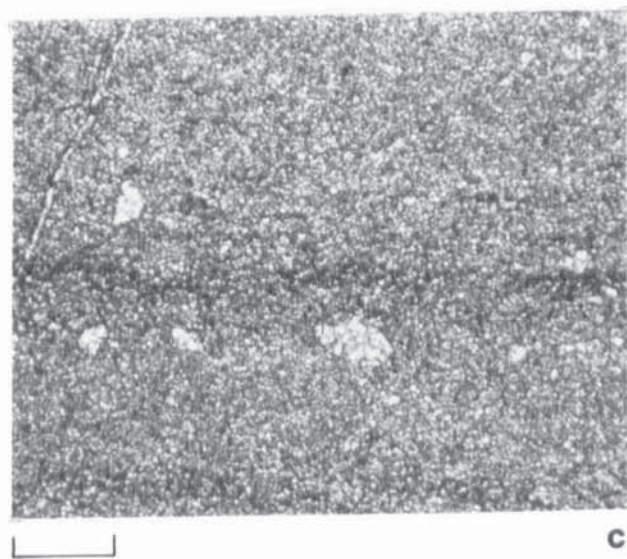
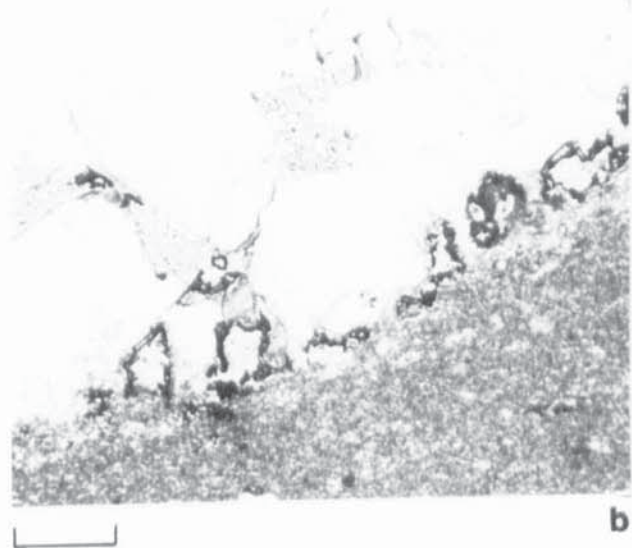
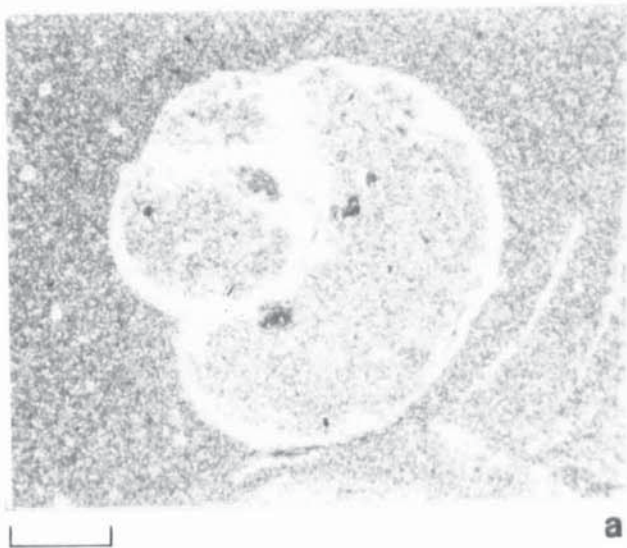
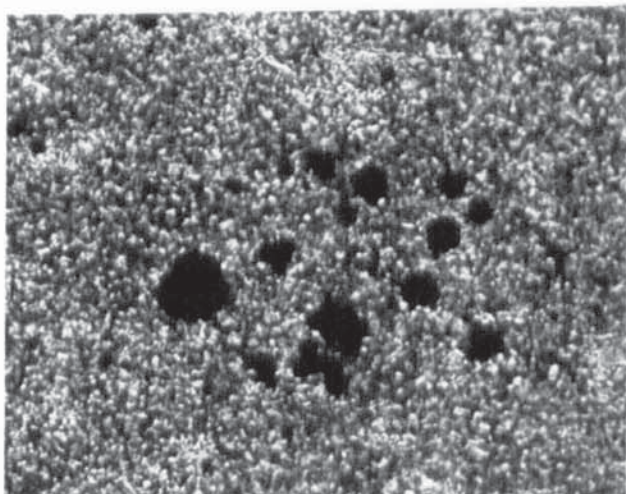


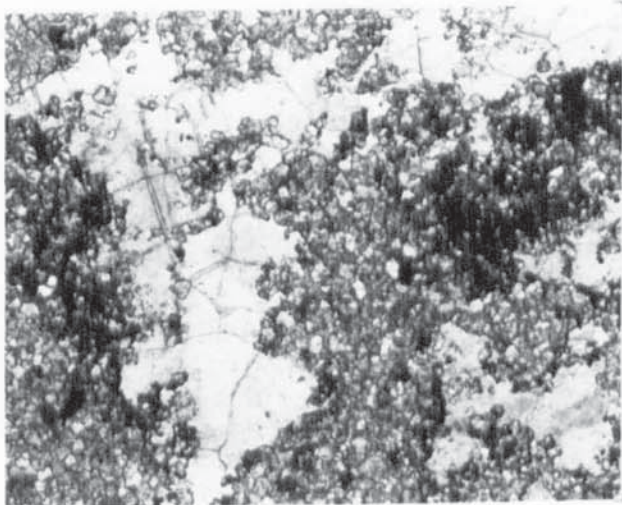
PLATE 7.5

- a) CM1: Aggregate of frambooidal pyrite in calciferous non-ferroan dolomite.  
Scale bar = 0.5mm
- b) MA101: Irregular patch of coarse grained non-ferroan calcite. Fine grained iron oxide is also present at the margins of the patch.  
Scale bar = 0.5mm
- c) MQ9: Small euhedral grains of titanium oxide. Viewed in reflected light.  
Scale bar = 40 $\mu$ m
- d) MQ9: Detrital haematite grain with authigenic overgrowth.  
Viewed in reflected light.  
Scale bar = 40 $\mu$ m
- e) MQ8: Dissolved carbonate veinlet containing abundant fine grained iron oxide.  
Scale bar = 0.1mm
- f) T1: Euhedral secondary void containing fine grained iron oxide.  
Scale bar = 0.5mm

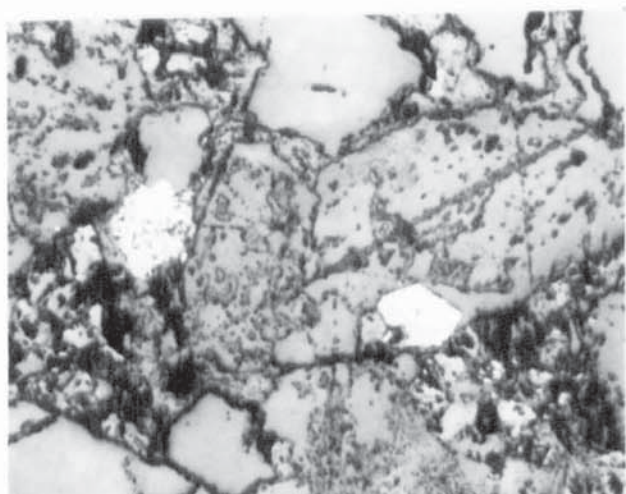
**Plate 7.5**



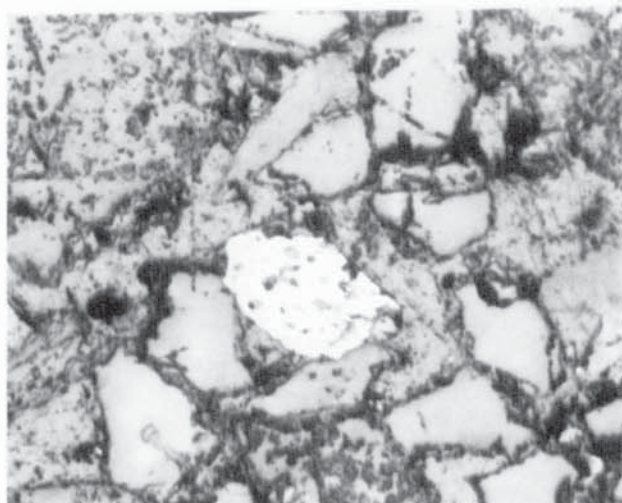
a



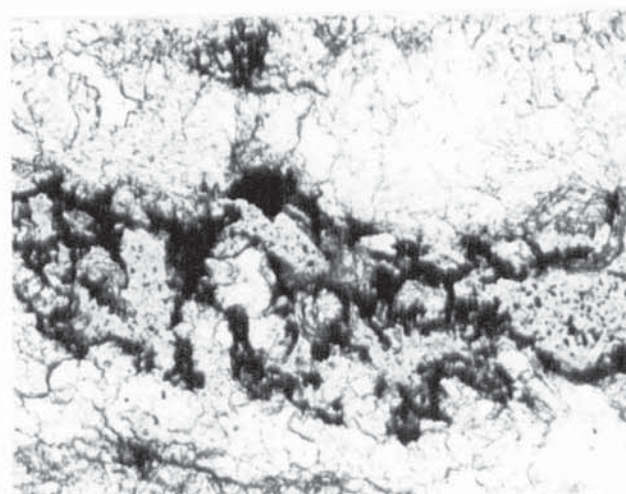
b



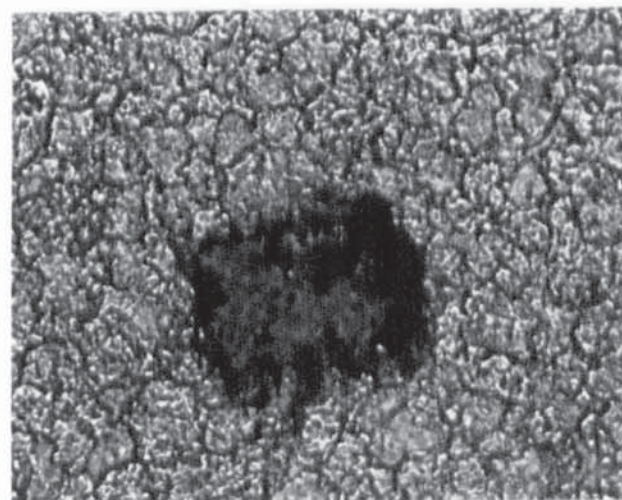
c



d



e



f

APPENDIX I

TABLE 9.1 Listing of techniques used on each sample.

SAMPLE	DIAGENESIS					PALAEOMAGNETISM					
	Thin Section	Point Count	Polished Block/Sec	XRD	SEM	NRM	Thermal (AF) Demag	Chemical Demag	IRM	Bulk Demag	Temp.(°C)
RG1	X	-	X	-	-	X	X	-	X	400	
RG2	X	-	-	X	X	X	X	-	-	400	
RG3	-	-	-	-	X	X	X	-	-	400	
RG4	X	-	-	-	-	X	(AF)	-	-	-	
RG5	X	-	X	X	X	X	X	-	X	400	
RG6	X	-	-	-	-	X	X	-	-	400	
RG7	X	-	-	-	-	X	X	-	-	400	
RG8	-	-	-	-	-	-	-	-	-	-	
RG9	-	-	-	-	-	-	-	-	-	-	
RG10	-	-	-	-	-	-	-	-	-	-	
RG11	X	-	-	-	-	X	X(AF)	-	-	-	
RG12	X	-	-	-	-	-	-	-	-	-	
RG13	X	-	X	-	-	X	X	-	-	300	
RG14	X	-	-	-	-	X	X	-	-	400	
RG15	-	-	-	-	-	X	X	-	-	400	
P1	X	X	-	-	-	X	X	-	-	500	
P2	-	-	-	-	-	X	X	-	-	500	
P3	X	X	-	X	X	X	X	-	X	400	
P4	-	-	-	-	-	X	X	-	-	400	
P5	X	X	-	-	-	X	X	-	-	400	
P6	-	-	-	-	-	X	X	-	-	580	
P7	X	X	X	-	X	X	X	-	-	630	
P8	X	X	X	X	X	X	X	-	-	580	
P9	X	-	X	-	-	X	X	X	X	580	
P10	X	X	-	-	-	X	X	-	-	580	
TA1	X	-	-	-	-	X	X	-	X	580	
TA2	X	X	-	-	-	X	X	-	-	660	
TA3	X	X	-	-	-	X	X	-	-	630	
TA4	X	X	-	X	X	X	X	-	-	630	
TA5	-	-	X	-	-	X	X	-	X	500	

Table 9.1 continued.

SAMPLE	DIAGENESIS					PALAEOMAGNETISM				
	Thin Section	Point Count	Polished Block/Sec	XRD	SEM	NRM	Thermal (AF) Demag	Chemical Demag	IRM	Bulk Demag
TA6	X	X	X	-	-	X	X	X	-	630
TA7	X	X	-	-	X	X	X	-	-	630
TA8	X	X	-	X	X	X	X	-	-	630
PN1	X	-	-	-	-	X	X	-	-	400/675
PN2	-	-	-	-	-	X	X	-	X	660
PN3	X	-	-	X	X	X	-	-	X	660
PN4	X	-	X	-	-	X	X	X	-	660
PN5	-	-	-	-	-	X	X	-	-	660
MA112	X	-	X	X	X	X	X	-	-	510
MA113	-	-	-	-	-	-	X	-	X	-
MA114	-	-	-	X	-	X	X	-	-	630/650
MA115	X	-	X	X	X	X	X	-	-	630/650
MA116	X	-	X	X	X	X	X	-	-	650
MA1	X	X	X	-	-	X	X	X	X	400
MA2	X	X	X	-	X	X	(AF)	-	-	-
MA3	-	-	-	-	-	X	X+(AF)	-	-	600
MA4	-	-	-	-	-	X	X	-	-	400
MA5	-	-	-	-	-	X	X	-	-	600
MA6	X	-	-	X	-	X	-	-	-	600
MA7	X	-	X	X	-	X	X	-	X	675
MA8	X	-	X	-	X	X	X	-	-	630
MA9	X	-	-	-	-	X	X	-	-	630
MA10	X	-	X	X	X	X	-	-	-	-
MA11	-	-	X	-	-	X	X	-	-	640
MA12	X	-	X	X	X	X	X	-	-	650
MA13	X	-	X	X	-	X	X	-	-	640
MA41	X	-	X	-	-	X	X	-	-	580
MA42	-	-	-	-	-	X	(AF)	-	-	660
MA43	X	-	X	-	-	X	X	-	-	550
MA44	X	-	X	-	-	X	(AF)	-	-	580
MA45	X	-	X	-	-	X	X	-	-	300
MA46	-	-	-	-	-	X	X	-	-	300

Table 9.1 continued.

SAMPLE	DIAGENESIS					PALAEOMAGNETISM				
	Thin Section	Point Count	Polished Block/Sec	XRD	SEM	NRM	Thermal (AF) Demag	Chemical Demag	IRM	Bulk Demag
MA47	-	-	-	-	-	-	-	-	-	-
MA48	X	-	-	-	-	X	X	-	-	630
MA49	-	-	X	-	-	X	X	-	-	630
MA50	-	-	-	-	-	X	X	-	-	630
MA51	X	-	X	X	-	X	X	-	X	640
MA52	X	-	X	X	-	X	X	-	-	600
MA53	X	-	X	-	-	X	X	X	X	675
MA54	-	-	-	-	-	X	X	-	-	675
MA55	-	-	-	-	-	X	X	-	-	675
MA56	X	-	-	X	X	-	-	-	-	-
MA57	X	-	-	-	-	X	X	-	-	400
MA58	X	-	X	-	-	X	X	-	-	580
MA59	-	-	-	-	-	X	X	-	-	580
MA60	-	-	-	-	-	X	(AF)	-	X	300
MA61	X	-	-	-	-	X	X	-	-	300
MA62	X	-	-	-	X	X	X	-	X	630
MA63	X	-	X	X	X	X	X	-	-	580
MA64	X	-	-	-	-	X	X	-	-	400
MA65	-	-	-	-	-	X	X	-	X	300
MA66	-	-	X	-	-	X	X	-	-	-
MA67	X	-	X	-	-	X	X	-	-	500
MA68	X	-	-	-	X	X	(AF)	-	-	-
MA69	X	-	-	-	-	X	X	-	-	675
MA70	-	-	-	-	-	X	(AF)	-	-	300
MA71	X	-	X	X	X	X	X	-	-	-
MA72	X	-	X	X	-	X	X	-	-	-
MA73	X	-	-	-	X	X	X	-	-	630
MA74	X	-	-	-	-	X	X	X	-	630
MA75	-	-	-	-	-	X	X	-	X	675
MA76	X	-	X	-	X	X	(AF)	-	-	580
MA77	X	-	X	X	-	X	X	-	-	-
MA78	X	-	-	X	X	X	X	-	-	630
MA79	-	-	-	-	-	X	X	-	-	400
MA80	X	-	X	X	X	X	-	-	-	-

Table 9.1 continued.

SAMPLE	DIAGENESIS					PALAEOMAGNETISM				
	Thin Section	Point Count	Polished Block/Sec	XRD	SEM	NRM	Thermal (AF) Demag	Chemical Demag	IRM	Bulk Demag
MA81	X	-	-	-	X	X	X	-	-	-
MA82	-	-	-	-	-	X	X	-	-	630
MA83	X	-	X	X	X	X	X	-	-	-
MA84	X	-	-	-	-	X	X	-	X	-
MA85	-	-	-	-	-	X	X	-	-	630
MA86	-	-	-	-	-	X	X	-	-	630
MA87	X	-	-	-	X	X	X	-	X	630
MA88	-	-	-	-	-	X	X	-	-	630
MA89	X	-	-	-	-	X	X	-	-	630
MA90	X	-	-	X	-	X	X	-	-	400
MA91	X	-	X	-	X	X	(AF)	-	-	-
MA92	X	-	X	-	-	X	(AF)	-	-	400
MA93	X	-	X	X	X	X	X	-	-	-
MA94	X	-	-	X	-	X	X	-	-	630
MA95	X	-	-	X	X	X	X	-	-	-
RA1	X	-	-	-	-	X	X	-	-	630
RA2	X	-	-	-	-	X	X	-	-	630
RA3	-	-	-	-	-	X	X	-	-	630
RA4	-	-	-	-	-	X	X	-	-	630
RA5	X	-	X	-	-	X	X	-	-	630
RA6	X	-	X	X	-	X	X	-	-	660
RA7	X	-	X	-	-	X	X	X	-	660
RA8	X	-	-	-	-	X	X	-	-	660
RA9	X	-	-	X	X	X	X	-	X	660
RA10	X	-	X	-	-	X	X	-	-	675
CM1	X	-	-	-	-	X	X+(AF)	-	X	-
CM2	-	-	-	-	-	-	-	-	-	-
CM3	X	-	-	-	X	X	X	-	-	300
CM4	-	-	-	-	-	X	X+(AF)	-	X	-
CM5	-	-	-	-	-	X	X	-	-	300

Table 9.1 continued.

SAMPLE	DIAGENESIS					PALAEOMAGNETISM					
	Thin Section	Point Count	Polished Block/Sec	XRD	SEM	NRM	Thermal (AF) Demag	Chemical Demag	IRM	Bulk Demag	Temp. (°C)
MA96	X	-	-	-	-	X	X+(AF)	-	X	-	-
MA97	X	-	-	-	-	X	X	-	-	-	500
MA98	-	-	-	-	-	X	X	-	X	500	
MA99	X	-	-	-	-	X	X	-	-	-	-
MA100	-	-	-	-	-	X	X	-	-	-	300
MA101	X	-	-	-	-	X	X	-	-	-	300
MA102	X	-	-	-	-	X	X	-	-	-	300
MA103	X	-	-	-	-	X	X	-	X	300	
MA104	-	-	-	-	-	X	X	-	-	-	-
MA105	X	-	-	-	-	X	X	-	-	-	300
MA106	-	-	-	-	-	X	X	-	-	-	300
MA107	-	-	-	-	-	X	X	-	-	-	300
MA108	X	-	-	-	-	X	X	-	-	-	300
MA109	-	-	-	-	-	X	X	-	-	-	300
MA110	-	-	-	-	-	X	X	-	-	-	300
MA111	X	-	X	-	-	X	X	-	X	300	
MQ1	-	-	-	-	-	X	X	-	-	-	-
MQ2	-	-	-	-	-	X	X+(Af)	-	-	-	-
MQ3	-	-	-	-	-	X	X	-	-	-	-
MQ4	X	-	-	-	-	X	(AF)	-	X	-	-
MQ5	X	X	-	X	-	X	X	-	-	-	-
MQ6	-	-	-	-	-	X	X	-	-	-	-
MQ7	X	X	-	-	-	X	-	-	-	-	-
MQ8	X	-	-	-	-	X	(AF)	-	-	-	-
MQ9	X	-	X	-	-	X	X	-	X	-	-
T1	X	-	-	X	-	X	(AF)	-	-	-	-
T2	X	-	-	-	-	X	X	-	X	300	
T3	X	-	X	-	-	X	X	-	-	-	300
T4	X	-	-	-	-	X	X	-	-	-	300

TOTAL  
156

Sample Preparation for Palaeomagnetic Analysis

Hand samples may be oriented by finding a flat surface on the sample, prior to removal. A horizontal line (strike) can then be marked on it, and converted into an arrow (conventionally with the maximum slope of the surface  $90^\circ$  clockwise from the arrow). The direction of the strike arrow, relative to true north, is then determined and the maximum amount of dip of the surface measured from horizontal. Where no flat surface is present, then a flat surface can be provided by gluing a plastic disk to the sample, and orienting the surface of the disk, or a tripod can be placed on the surface (Fig. 9.1) the legs of which are marked on the sample and the strike and dip of the surface of the tripod are then measured.

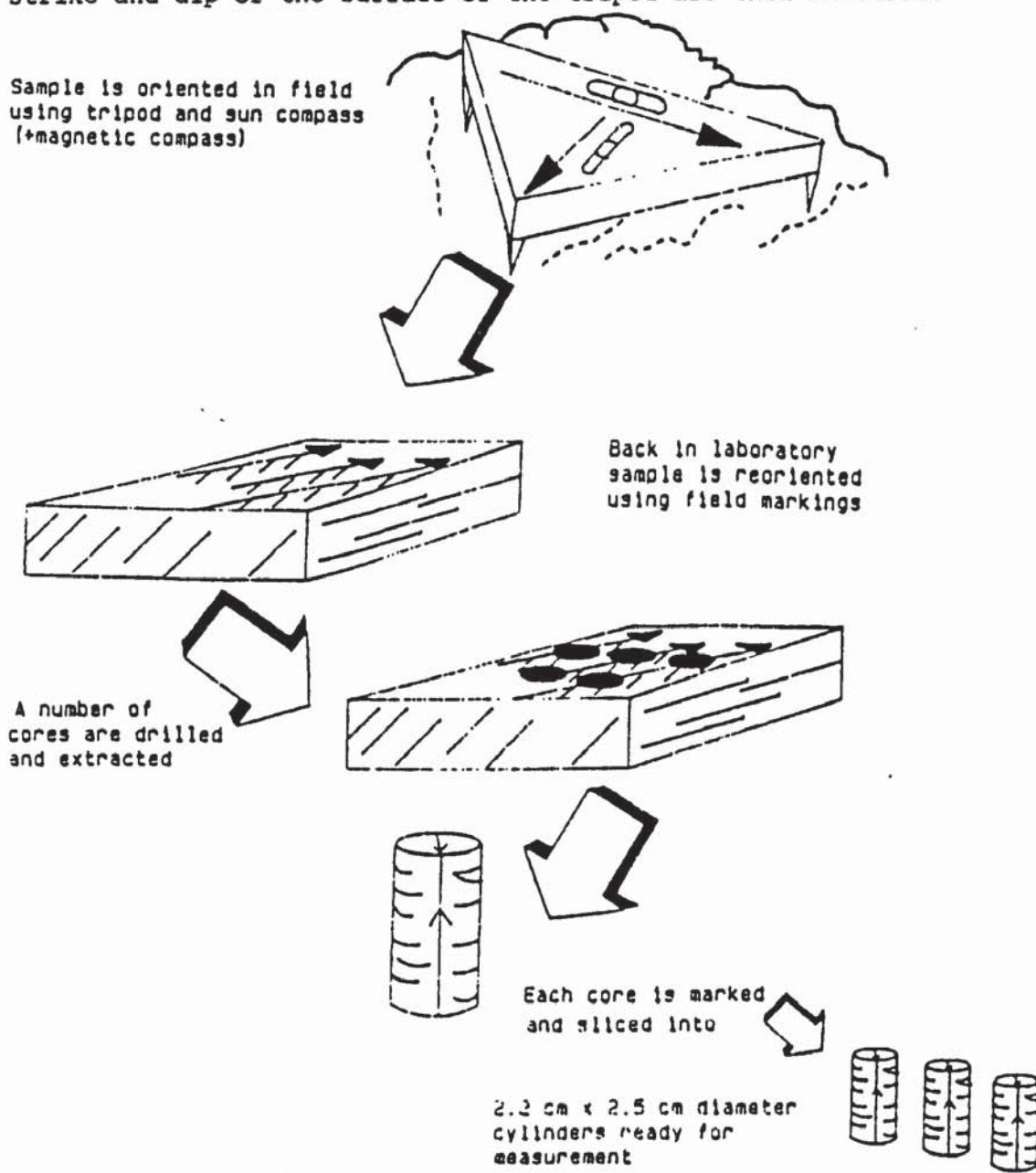


Fig. 9.1 Shows how sample is orientated in the field and how it is prepared for palaeomagnetic measurement.

### APPENDIX III

#### Staining a Thin Section

1. Prepare a  $<3\mu\text{m}$  thin section of the rocks but omit the coverslip.  
Ensure that no dirt or grease adheres to the surface.
2. Prepare two staining solutions:
 

Solution A: Alizarin Red S - concentration of 0.2 g/100 ml of 1.5% hydrochloric acid (15 ml pure acid made up to 1 litre with water).

Solution B: Potassium ferricyanide - concentration 2 g/100 ml of 1.5% hydrochloric acid.
3. Mix solutions A and B in the proportion 3 parts by volume of A to 2 parts of B.
4. Immerse the thin section in the mixture of solutions for 30-45 seconds, agitating gently for at least part of the time to remove gas bubbles from the surface.
5. Wash the stained section in running water for a few seconds.
6. Allow to dry.
7. Cover with polyurethane varnish or a coverslip in the normal way.

Note: The solution of Alizarin Red S in acid may be made up beforehand and will keep, but the potassium ferricyanide must be made fresh each time. A large number of sections can be stained with 250 ml of stain solution.

**Table 9.2 Etching and staining characteristics of carbonate minerals**

Mineral	Effect of etching	Stain colour with Alizarin Red S	Stain colour with potassium ferricyanide	Combined result
Calcite (non-ferroan)	Considerable (relief reduced)	Pink to red-brown	None	Pink to red-brown
Calcite (ferroan)	Considerable (relief reduced)	Pink to red-brown	Pale to deep blue depending on iron content	Mauve to blue
Dolomite (non-ferroan)	Negligible (relief maintained)	None	None	Colourless
Dolomite (ferroan)	Negligible (relief maintained)	None	Very pale blue	Very pale blue (appears turquoise or greenish in thin section)

APPENDIX IV

Classification of Terrigenous Sandstones (after Dott, 1964)



Fig. 9.2 Classification of terrigenous sandstones (after Dott, 1964).

## APPENDIX V

### (a) The Preparation of Orientated Clay Mineral Specimens for X-Ray Diffraction Analysis by a Suction-onto-Ceramic Tile Method

Suction-onto-ceramic tile methods involve filtering a clay suspension under suction through a ceramic medium so that the clay material is deposited on the ceramic. The particular method described here uses a stainless steel filter funnel (e.g. a Gallenkamp FD-350) with ceramic disc filter beds from 1.5 in. (37.3 mm) in diameter and  $\frac{1}{8}$  in. (6.2 mm) thick. The ceramic disc filter beds are drilled with a rock corer from standard unglazed biscuit tiles (manufactured by Richard Tiles of Tunstall, Stoke-on-Trent. Ideally the ceramic medium should allow about 100 mg/in.<sup>2</sup> of clay material to be deposited within about 5-10 min to prevent segregation effects. The method requires no modification of the X-ray diffractometer. The ceramic discs are sufficiently thin to be inserted and securely held by the specimen holder clip. They are also of a sufficiently large diameter for the X-ray beam always to lie within the area covered by the specimen.

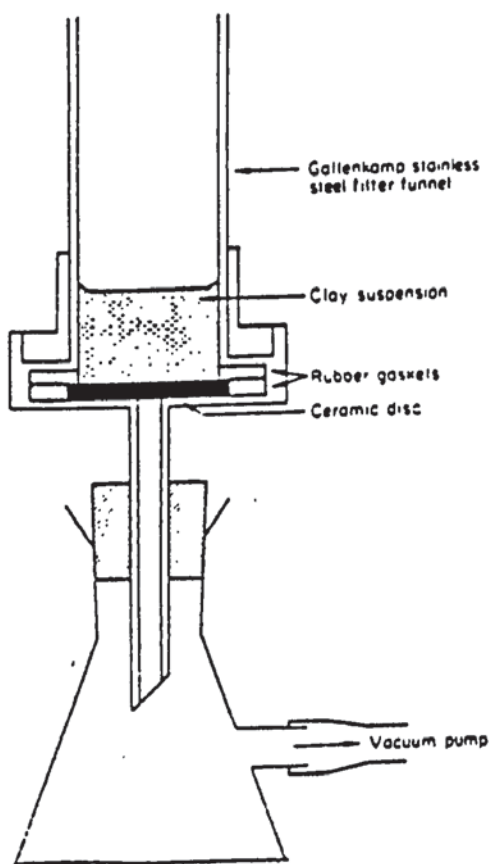


Fig. 9.3 Suction-onto-ceramic disc method of sample preparation.

## APPENDIX V

### (b) Identification of X-ray diffraction peaks.

Table 9.3 Key to identification of X-ray diffractogram peaks.

- A: Analcime
- B: Barite
- C: Chlorite
- Ca: Calcite
- Cp: Clinoptilolite
- D: Dolomite
- F: Feldspar
- G: Goethite
- H: Haematite
- I: Illite
- K: Kaolinite
- M: Montmorillonite
- P: Plagioclase feldspar
- Q: Quartz
- S: Smectite
- Si: Siderite

APPENDIX VI

Table 9.4 Types of magnetization (after Tarling, 1983)

Remanent type of magnetization	Abbreviation	Characteristic or definition
<u>Naturally occurring magnetizations</u>		
Natural	NRM	Summation of all components of specimen remanence acquired by natural processes.
Thermal	TRM	Acquired by cooling over a range of temperatures at or below the Curie temperature.
Depositional/detrital	DRM	Acquired by the physical rotation of magnetic particles during deposition as a sediment.
Post-depositional	DDRM	Acquired by sediments after deposition but prior to metamorphism or weathering; usually a combination of physical rotation of interstitial particles and chemical changes as sediments consolidate.
Chemical	CRM	Acquired as a magnetic mineral nucleates and grows in a magnetic field.
Shear	SRM	Acquired mostly by unconsolidated sediments when subjected to shear.
<u>Laboratory-induced magnetization</u>		
Isothermal	IRM	Acquired by magnetic particles in steady magnetic field in a few seconds; the field is generally strong. This can also be acquired naturally in lightning strikes.
Anhysteretic	ARM	Acquired when a ferromagnetic particle subjected simultaneously to alternating and direct magnetic fields.
Rotational	RRM	Acquired by a specimen rotating within an alternating magnetic field.
Gyromagnetic	GRM	Acquired by a specimen in an alternating magnetic field without rotation.
Shock	SRM	Acquired by magnetic particles when shocked by impact. This can also occur naturally such as during meteoritic impacts.

APPENDIX VII

POINT COUNT ANALYSIS FOR THE AUTUNIAN OF PALMACES

TABLE 9.5  
(1000 POINTS COUNTED FOR  
EACH SAMPLE)

	<u>P1</u>	<u>P3</u>	<u>P5</u>	<u>P7</u>	<u>P8</u>	<u>P10</u>
QUARTZ (MONOCRYSTALLINE)	1.7	24.0	8.2	18.1	12.0	21.0
QUARTZ (STRAINED)	2.7	3.4	7.3	1.6	1.2	2.5
QUARTZ (POLYCRYSTALLINE)	0.3	5.4	19.0	12.5	11.2	5.8
FELDSPAR (PLAGIOCLASE)	-	0.2	0.4	0.2	0.4	0.2
FELDSPAR (POTASSIUM)	1.7	4.7	14.8	1.2	2.8	0.7
ROCK FRAGMENTS (SED)	-	5.8	-	8.7	11.6	1.1
ROCK FRAGMENTS (IGN)	65.0	1.7	1.1	2.4	9.2	2.2
ROCK FRAGMENTS (MET)	-	2.4	2.9	4.7	10.0	3.3
ROCK FRAGMENTS (ALT- CLAY)	0.3	1.0	3.7	0.8	2.0	0.7
ROCK FRAGMENTS (ALT- Fe <sub>2</sub> O <sub>3</sub> )	-	-	0.3	4.0	11.6	1.8
MICA (MUSCOVITE)	8.7	2.0	2.9	0.8	0.4	4.3
MICA (BIOTITE)	1.3	1.4	1.1	-	0.4	0.4
MICA (ALT- CLAY)	-	-	-	4.3	1.4	-
HEAVY/ACCOSSORY MINERALS	3.0	1.4	-	0.4	0.4	0.4
OPAQUES (FINE GRAINED)	1.0	1.4	6.9	14.2	6.8	5.1
OPAQUES (COARSE)	1.7	2.0	1.1	7.6	6.4	11.2
CLAY (ILLITE/MIXED LAYER I-S SMECTITE/CHLORITE)	-	6.4	12.8	0.8	0.8	20.2
CLAY (KAOLINITE)	11.0	3.1	8.4	-	2.4	1.4
CEMENT (QUARTZ)	-	3.7	1.2	2.0	0.4	0.4
CEMENT (K. FELDSPAR)	-	-	-	-	-	-
CEMENT (NON Fe. DOLOMITE)	0.3	20.0	4.5	8.3	4.2	11.5
CEMENT (Fe. DOL/ANK/SID)	-	9.8	1.6	5.1	2.8	5.5
CEMENT (NON Fe. CALCITE)	0.2	0.1	0.2	1.2	-	-
CEMENT (Fe. CALCITE)	-	-	-	-	-	-
CEMENT (BARITE)	-	-	-	-	-	-
VISIBLE POROSITY	0.3	0.1	1.8	1.6	0.8	0.4
TOTAL%	99.2	100.0	100.2	100.0	99.7	100.1
AVE. GRAIN SIZE (MM)	0.04	0.13	0.35	0.19	0.21	0.12

## APPENDIX VII

### POINT COUNT ANALYSIS FOR THE SAXONIAN

TABLE 9.6  
(1000 POINTS COUNTED FOR  
EACH SAMPLE)

	<u>MA112</u>	<u>MA115</u>	<u>MA116</u>	<u>PN1</u>	<u>PN3</u>	<u>PN4</u>	<u>TA2</u>	<u>TA3</u>	<u>TA4</u>	<u>TA6</u>	<u>TA7</u>	<u>TA8</u>
QUARTZ (MONOCRYSTALLINE)	51.6	45.6	37.0	32.0	22.0	33.3	28.0	28.7	32.0	36.8	32.8	36.9
QUARTZ (STRAINED)	10.7	2.8	3.6	7.0	9.3	6.0	9.6	5.2	3.2	4.8	1.6	3.1
QUARTZ (POLYCRYSTALLINE)	1.0	4.3	5.9	7.0	3.5	7.2	4.7	7.1	6.0	6.1	8.2	5.1
FELDSPAR (PLAGIOCLASE)	-	0.1	0.1	0.2	0.1	-	-	-	0.1	-	-	-
FELDSPAR (POTASSIUM)	3.0	3.0	0.5	6.4	6.0	1.0	7.6	4.8	8.0	5.8	2.5	4.7
ROCK FRAGMENTS (SED)	0.3	2.0	3.2	0.3	1.3	-	-	1.6	0.5	-	1.6	0.7
ROCK FRAGMENTS (IGN)	0.3	0.8	0.4	1.0	1.4	1.0	1.3	1.6	2.8	0.8	2.3	1.3
ROCK FRAGMENTS (MET)	0.3	-	-	1.6	0.7	1.3	0.7	0.5	-	0.4	-	1.0
ROCK FRAGMENTS (ALT- CLAY)	1.3	-	-	3.5	4.0	1.6	1.7	0.9	0.6	0.5	2.8	2.3
ROCK FRAGMENTS (ALT- Fe <sub>2</sub> O <sub>3</sub> )	-	0.4	0.5	-	-	-	2.0	1.5	1.2	0.7	0.5	2.0
MICA (MUSCOVITE)	0.5	0.4	0.5	1.7	1.8	0.6	1.7	1.3	2.0	1.5	2.0	1.3
MICA (BIOTITE)	-	-	-	0.7	1.3	0.3	0.3	0.8	0.1	0.8	0.8	0.3
MICA (ALT- CLAY)	-	-	-	-	-	-	-	0.8	0.4	-	0.9	-
HEAVY/ACCOSSORY MINERALS	0.3	0.8	-	0.7	-	-	-	0.8	0.8	1.2	0.7	0.3
OPAQUES (FINE GRAINED)	15.4	18.4	23.3	8.8	9.0	23.6	14.6	17.4	12.0	21.5	14.0	9.1
OPAQUES (COARSE)	-	0.8	2.0	0.1	2.0	4.2	0.9	2.0	1.2	1.6	0.5	0.3
CLAY (ILLITE/MIXED LAYER I-S SMECTITE/CHLORITE)	1.3	0.7	0.9	12.3	3.3	5.1	8.6	0.8	3.2	2.0	6.9	8.4
CLAY (KAOLINITE)	1.8	-	0.4	3.2	1.7	0.3	2.3	2.8	4.5	3.2	3.8	1.8
CEMENT (QUARTZ)	9.3	18.3	11.0	13.0	9.9	13.0	9.0	14.1	17.3	8.8	11.0	12.5
CEMENT (K. FELDSPAR)	-	-	-	-	-	-	0.3	-	0.8	0.8	0.9	0.3
CEMENT (NON Fe. DOLOMITE)	-	-	-	-	15.0	-	0.9	1.3	2.8	1.1	1.2	2.6
CEMENT (Fe. DOL/ANK/SID)	0.5	0.4	0.5	-	-	0.9	0.2	0.4	0.9	0.1	0.2	0.9
CEMENT (NON Fe. CALCITE)	0.1	-	-	-	2.0	-	-	-	-	-	-	-
CEMENT (Fe. CALCITE)	-	-	-	-	-	-	-	-	-	-	-	-
CEMENT (BARITE)	0.5	-	0.9	-	-	-	-	-	-	-	-	-
VISIBLE POROSITY	1.8	1.2	6.3	0.5	6.0	0.5	5.6	5.5	3.6	1.6	4.7	2.3
TOTAL%	100.0	100.0	100.0	100.2	100.1	99.9	100.0	100.0	100.0	100.1	99.9	99.8
AVE. GRAIN SIZE (MM)	0.25	0.17	0.16	0.16	0.15	0.16	0.16	0.16	0.16	0.13	0.16	0.26

APPENDIX VII

POINT COUNT ANALYSIS FOR THE LOWER BUNTSANDSTEIN

TABLE 9.7  
(1000 POINTS COUNTED FOR  
EACH SAMPLE)

	<u>MA1</u>	<u>MA6</u>	<u>MA7</u>	<u>MA8</u>	<u>MA9</u>	<u>MA10</u>	<u>MA12</u>	<u>MA13</u>	<u>MA41</u>	<u>MA44</u>	<u>MA45</u>	<u>MA48</u>
QUARTZ (MONOCRYSTALLINE)	28.1	33.4	33.5	30.0	24.5	21.3	31.0	31.3	28.4	26.9	37.8	42.6
QUARTZ (STRAINED)	4.0	3.2	1.6	3.4	1.3	3.6	3.3	4.8	4.0	3.3	2.1	4.8
QUARTZ (POLYCRYSTALLINE)	10.9	8.8	8.4	14.1	19.8	17.3	7.5	12.0	16.2	13.5	13.4	10.9
FELDSPAR (PLAGIOCLASE)	-	0.2	0.2	0.1	0.1	0.2	0.3	0.3	0.2	0.2	0.2	0.1
FELDSPAR (POTASSIUM)	1.4	12.1	10.1	6.0	6.1	4.5	12.5	12.0	10.3	8.4	10.7	4.8
ROCK FRAGMENTS (SED)	-	0.8	0.4	0.3	2.0	4.9	3.0	2.8	3.2	1.3	1.7	3.2
ROCK FRAGMENTS (IGN)	0.5	0.8	1.2	1.0	0.4	2.0	5.6	2.4	0.4	1.3	1.7	1.2
ROCK FRAGMENTS (MET)	1.5	2.0	0.4	0.3	3.2	1.2	3.0	1.6	3.2	2.3	2.3	0.8
ROCK FRAGMENTS (ALT- CLAY)	1.0	0.8	0.8	2.8	2.8	3.2	2.2	0.4	1.0	2.5	1.0	-
ROCK FRAGMENTS (ALT- Fe <sub>2</sub> O <sub>3</sub> )	-	-	-	0.1	1.2	5.3	0.1	0.4	0.6	-	-	-
MICA (MUSCOVITE)	1.3	1.6	1.6	0.7	1.5	0.4	1.5	2.0	0.8	1.8	1.0	0.4
MICA (BIOTITE)	0.1	0.2	0.2	0.1	0.8	0.8	0.8	0.4	0.1	2.8	0.7	0.4
MICA (ALT- CLAY)	-	0.2	0.4	0.1	0.8	0.1	0.1	0.4	0.8	0.2	0.2	1.2
HEAVY/ACCOSSORY MINERALS	0.7	-	-	0.7	0.4	-	0.3	0.8	0.4	-	1.3	0.2
OPAQUES (FINE GRAINED)	4.9	7.2	1.0	3.7	7.1	7.6	5.2	0.4	0.8	2.5	-	4.8
OPAQUES (COARSE)	0.3	1.2	0.3	0.7	3.2	5.3	0.7	1.6	0.8	0.9	1.0	1.6
CLAY (ILLITE/MIXED LAYER I-S SMECTITE/CHLORITE)	10.5	3.1	3.3	10.0	7.1	2.4	9.2	4.3	4.6	11.9	5.0	7.8
CLAY (KAOLINITE)	9.9	4.4	4.0	5.0	2.1	2.8	2.3	4.4	3.2	2.3	2.3	4.0
CEMENT (QUARTZ)	18.8	14.4	15.7	18.4	11.3	14.6	10.0	13.3	16.0	10.1	12.4	6.4
CEMENT (K. FELDSPAR)	0.1	0.4	-	0.2	-	-	-	1.6	1.6	0.4	-	-
CEMENT (NON Fe. DOLOMITE)	-	-	-	-	-	-	-	-	-	-	-	-
CEMENT (Fe. DOL/ANK/SID)	-	-	-	-	-	-	-	-	-	-	-	-
CEMENT (NON Fe. CALCITE)	-	-	-	-	-	-	-	-	-	-	-	-
CEMENT (Fe. CALCITE)	-	-	-	-	-	-	-	-	-	-	-	-
CEMENT (BARITE)	-	-	-	-	-	-	-	-	-	-	-	-
VISIBLE POROSITY	7.9	5.6	16.7	2.9	4.0	2.8	1.9	2.8	3.6	7.4	4.9	4.8
TOTAL%	99.4	100.4	99.8	100.6	99.7	100.3	100.5	100.0	100.2	100.0	99.7	100.0
AVE. GRAIN SIZE (MM)	0.28	0.36	0.28	0.33	0.31	0.28	0.61	0.42	0.37	0.28	0.33	0.26

CONTINUED .....

## APPENDIX VII

### POINT COUNT ANALYSIS FOR THE LOWER BUNTSANDSTEIN

TABLE 9.7 (CONTINUED ....)  
 (1000 POINTS COUNTED FOR  
 EACH SAMPLE)

	<u>MA51</u>	<u>MA52</u>	<u>MA53</u>	<u>MA56</u>	<u>MA57</u>
QUARTZ (MONOCRYSTALLINE)	44.7	42.6	38.0	30.3	19.9
QUARTZ (STRAINED)	2.4	2.4	3.4	4.6	4.6
QUARTZ (POLYCRYSTALLINE)	6.9	13.3	10.4	8.6	6.6
FELDSPAR (PLAGIOCLASE)	0.2	0.1	0.1	0.2	-
FELDSPAR (POTASSIUM)	12.6	5.4	10.7	12.7	6.9
ROCK FRAGMENTS (SED)	2.4	1.6	0.2	2.7	0.8
ROCK FRAGMENTS (IGN)	0.4	0.8	0.6	0.3	1.2
ROCK FRAGMENTS (MET)	0.8	0.2	2.0	0.7	0.4
ROCK FRAGMENTS (ALT- CLAY)	0.8	-	0.2	1.0	0.8
ROCK FRAGMENTS (ALT- Fe <sub>2</sub> O <sub>3</sub> )	-	-	-	-	-
MICA (MUSCOVITE)	1.6	0.4	0.6	0.9	2.0
MICA (BIOTITE)	0.2	0.1	0.1	0.9	0.4
MICA (ALT- CLAY)	-	-	-	-	-
HEAVY/ACCOSSORY MINERALS	-	0.8	0.3	1.0	0.4
OPAQUES (FINE GRAINED)	2.0	4.0	0.8	10.0	0.6
OPAQUES (COARSE)	2.0	1.5	0.8	0.2	0.6
CLAY (ILLITE/MIXED LAYER I-S SMECTITE/CHLORITE)	1.8	2.0	2.3	2.6	4.0
CLAY (KAOLINITE)	4.8	3.2	3.0	1.0	2.4
CEMENT (QUARTZ)	10.0	12.0	17.7	13.5	2.4
CEMENT (K. FELDSPAR)	-	0.2	1.3	1.3	-
CEMENT (NON Fe. DOLOMITE)	-	-	-	-	35.8
CEMENT (Fe. DOL/ANK/SID)	-	-	-	-	2.8
CEMENT (NON Fe. CALCITE)	-	-	-	-	5.6
CEMENT (Fe. CALCITE)	-	-	-	-	-
CEMENT (BARITE)	-	-	-	-	-
VISIBLE POROSITY	6.4	8.0	7.2	7.3	1.6
TOTAL%	100.0	99.6	99.7	99.8	99.8
AVE. GRAIN SIZE (MM)	0.36	0.41	0.41	0.30	0.40

APPENDIX VII

POINT COUNT ANALYSIS FOR THE UPPER BUNDSENDSTEIN

TABLE 9.8  
(1000 POINTS COUNTED FOR  
EACH SAMPLE)

	<u>MA61</u>	<u>MA62</u>	<u>MA63</u>	<u>MA64</u>	<u>MA67</u>	<u>MA68</u>	<u>MA69</u>	<u>MA71</u>	<u>MA72</u>	<u>MA74</u>	<u>MA80</u>	<u>MA83</u>
QUARTZ (MONOCRYSTALLINE)	54.0	32.7	30.1	41.0	32.0	32.0	28.3	28.9	33.4	39.0	36.0	34.0
QUARTZ (STRAINED)	2.8	2.0	0.8	3.6	2.9	2.4	5.2	3.7	6.4	5.0	2.0	6.4
QUARTZ (POLYCRYSTALLINE)	9.5	9.7	9.1	10.6	6.2	12.0	9.4	1.8	8.6	6.6	0.8	3.6
FELDSPAR (PLAGIOCLASE)	0.1	0.2	0.1	-	-	0.1	0.2	0.2	0.1	-	-	-
FELDSPAR (POTASSIUM)	5.2	10.6	11.0	12.8	10.9	16.0	9.6	11.9	9.0	7.3	5.6	4.4
ROCK FRAGMENTS (SED)	-	2.3	2.4	2.4	1.4	1.2	1.6	0.5	0.8	2.0	0.8	-
ROCK FRAGMENTS (IGN)	1.2	1.3	-	1.2	-	0.4	-	0.5	0.4	0.7	0.4	-
ROCK FRAGMENTS (MET)	1.8	1.7	0.8	1.6	1.4	1.6	1.5	0.5	1.1	2.7	-	-
ROCK FRAGMENTS (ALT- CLAY)	-	2.0	1.6	2.0	1.8	2.4	0.4	0.2	1.5	0.7	2.3	-
ROCK FRAGMENTS (ALT- Fe <sub>2</sub> O <sub>3</sub> )	-	-	-	-	-	-	2.4	-	0.8	0.3	0.5	-
MICA (MUSCOVITE)	0.5	4.7	1.0	0.8	3.6	1.2	1.2	1.2	1.8	0.3	1.6	6.8
MICA (BIOTITE)	0.5	0.7	0.4	0.3	-	0.3	0.9	-	-	0.2	0.3	1.2
MICA (ALT- CLAY)	-	0.7	1.2	0.4	0.7	-	1.2	-	1.1	-	-	-
HEAVY/ACCOSSORY MINERALS	0.4	0.3	-	-	0.8	0.4	1.1	0.5	0.8	0.3	0.5	-
OPAQUES (FINE GRAINED)	1.2	1.6	2.0	2.0	3.6	3.8	2.4	6.5	14.3	3.7	10.4	19.6
OPAQUES (COARSE)	0.8	1.0	0.2	0.8	0.2	0.4	1.6	0.9	0.4	1.0	0.8	8.0
CLAY (ILLITE/MIXED LAYER I-S SMECTITE/CHLORITE)	2.8	1.3	2.4	2.0	4.4	3.6	0.8	0.4	1.9	-	0.5	0.4
CLAY (KAOLINITE)	-	3.3	2.4	0.8	6.2	2.4	0.2	-	-	-	-	-
CEMENT (QUARTZ)	6.0	11.8	16.0	7.4	8.4	8.8	6.8	11.8	8.8	16.6	7.2	7.2
CEMENT (K. FELDSPAR)	0.6	1.8	1.2	0.4	0.4	2.4	0.8	3.6	-	0.3	1.5	-
CEMENT (NON Fe. DOLOMITE)	-	-	-	-	-	-	22.8	15.4	-	-	-	1.6
CEMENT (Fe. DOL/ANK/SID)	-	-	-	-	-	-	-	-	-	-	-	-
CEMENT (NON Fe. CALCITE)	-	-	-	-	-	-	-	-	-	-	-	-
CEMENT (Fe. CALCITE)	-	-	-	-	-	-	-	-	-	-	-	-
CEMENT (BARITE)	-	-	-	-	-	-	-	-	-	-	-	-
VISIBLE POROSITY	12.5	10.3	17.3	9.7	15.0	8.8	1.6	11.7	8.6	13.4	28.8	6.8
TOTAL%	99.9	100.0	100.0	99.8	99.9	100.2	100.0	100.0	100.0	100.1	100.0	100.0
AVE. GRAIN SIZE (MM)	0.37	0.33	0.29	0.28	0.27	0.39	0.29	0.19	0.19	0.26	0.09	0.09

CONTINUED ....

## APPENDIX VII

### POINT COUNT ANALYSIS FOR THE UPPER BUNDSSANDSTEIN

TABLE 9.8 (CONT.)  
 (1000 POINTS COUNTED FOR  
 EACH SAMPLE)

	<u>MA89</u>	<u>MA91</u>	<u>MA92</u>	<u>MA93</u>	<u>MA94</u>	<u>RA1</u>	<u>RA5</u>	<u>RA6</u>	<u>RA10</u>
QUARTZ (MONOCRYSTALLINE)	25.8	32.4	24.6	25.8	45.8	27.5	35.3	33.8	23.9
QUARTZ (STRAINED)	2.0	4.4	5.2	2.6	1.3	6.0	18.0	3.4	3.1
QUARTZ (POLYCRYSTALLINE)	2.4	5.6	5.2	4.0	-	5.7	0.4	2.8	5.2
FELDSPAR (PLAGIOCLASE)	-	0.2	-	-	-	0.3	0.2	0.3	-
FELDSPAR (POTASSIUM)	8.6	15.3	16.0	4.4	5.0	14.5	12.5	22.4	20.2
ROCK FRAGMENTS (SED)	0.4	0.4	1.2	-	0.5	0.4	-	-	1.0
ROCK FRAGMENTS (IGN)	-	0.4	0.4	-	-	0.2	-	-	-
ROCK FRAGMENTS (MET)	-	1.2	0.8	-	-	-	-	-	-
ROCK FRAGMENTS (ALT- CLAY)	0.4	0.4	0.8	1.2	-	0.4	-	0.8	1.0
ROCK FRAGMENTS (ALT- Fe <sub>2</sub> O <sub>3</sub> )	-	-	-	-	-	-	-	-	-
MICA (MUSCOVITE)	0.2	2.8	1.4	3.2	4.0	5.0	7.0	3.2	1.3
MICA (BIOTITE)	0.3	1.5	1.6	3.2	1.5	1.2	1.6	0.5	1.0
MICA (ALT- CLAY)	-	-	0.9	1.0	0.5	-	-	-	-
HEAVY/ACCESSORY MINERALS	0.3	-	-	-	-	0.8	0.4	0.5	0.5
OPAQUES (FINE GRAINED)	45.5	2.4	2.8	16.0	13.0	11.3	4.7	15.4	13.3
OPAQUES (COARSE)	4.3	2.0	1.0	4.7	2.0	1.8	1.2	0.5	1.0
CLAY (ILLITE/MIXED LAYER I-S SMECTITE/CHLORITE)	0.5	2.4	3.6	0.5	0.8	3.6	3.5	2.8	9.3
CLAY (KAOLINITE)	-	-	-	-	-	-	0.8	-	-
CEMENT (QUARTZ)	2.7	10.5	5.2	1.5	3.3	9.3	9.8	7.4	1.8
CEMENT (K. FELDSPAR)	0.3	3.6	5.6	0.5	0.8	2.5	1.6	2.8	7.1
CEMENT (NON Fe. DOLOMITE)	2.7	3.2	4.8	23.2	5.4	9.0	-	-	-
CEMENT (Fe. DOL/ANK/SID)	-	-	-	-	-	-	-	-	-
CEMENT (NON Fe. CALCITE)	3.0	-	-	-	-	-	-	-	-
CEMENT (Fe. CALCITE)	-	-	-	-	-	-	-	-	-
CEMENT (BARITE)	-	-	-	-	-	-	-	-	-
VISIBLE POROSITY	0.5	11.3	18.0	10.0	16.2	0.5	3.1	3.4	9.3
TOTAL%	99.9	100.0	99.9	100.0	100.1	100.0	100.1	100.0	100.0
AVE. GRAIN SIZE (MM)	0.10	0.14	0.13	0.05	0.05	0.10	0.05	0.13	0.21

## APPENDIX VII

### POINT COUNT ANALYSIS FOR THE MUSCHELKALK OF RIBA DE SANTIUSTE

TABLE 9.9  
(1000 POINTS COUNTED FOR  
EACH SAMPLE)

	<u>MQ5</u>	<u>MQ7</u>
QUARTZ (MONOCRYSTALLINE)	22.4	30.0
QUARTZ (STRAINED)	4.8	5.2
QUARTZ (POLYCRYSTALLINE)	0.4	1.2
FELDSPAR (PLAGIOCLASE)	0.2	0.4
FELDSPAR (POTASSIUM)	12.8	18.0
ROCK FRAGMENTS (SED)	-	1.6
ROCK FRAGMENTS (IGN)	-	-
ROCK FRAGMENTS (MET)	-	-
ROCK FRAGMENTS (ALT- CLAY)	0.8	0.8
ROCK FRAGMENTS (ALT- Fe <sub>2</sub> O <sub>3</sub> )	-	-
MICA (MUSCOVITE)	6.8	6.8
MICA (BIOTITE)	1.6	3.6
MICA (ALT- CLAY)	-	-
HEAVY/ACCOSSORY MINERALS	0.4	0.8
OPAQUES (FINE GRAINED)	8.0	4.8
OPAQUES (COARSE)	2.0	0.9
CLAY (ILLITE/MIXED LAYER I-S SMECTITE/CHLORITE)	3.6	5.7
CLAY (KAOLINITE)	-	2.8
CEMENT (QUARTZ)	7.6	10.1
CEMENT (K. FELDSPAR)	2.2	2.0
CEMENT (NON Fe. DOLOMITE)	12.8	-
CEMENT (Fe. DOL/ANK/SID)	-	-
CEMENT (NON Fe. CALCITE)	-	-
CEMENT (Fe. CALCITE)	-	-
CEMENT (BARITE)	-	-
VISIBLE POROSITY	13.6	5.6
TOTAL%	100.0	100.3
AVE. GRAIN SIZE (MM)	0.06	0.11

APPENDIX VIII

STABILITY INDEX (S.I.)

Subjective Estimations of Stability (Tarling, 1983)

Table 9.10

